RSC Advances

ROYAL SOCIETY OF CHEMISTRY

www.rsc.org/advances

Optimization of the process parameters for fabrication of polymer coated layered double hydroxide-methotrexate nanohybrid for possible treatment of osteosarcoma.

Sayantan Ray[a], Akhilesh Mishra[b], Tapan Kumar Mandal[b], Biswanath Sa[c] and Jui Chakraborty[a]

Received (in XXX, XXX) Xth XXXXXXXXX 20XX, Accepted Xth XXXXXXXXX 20XX
DOI: 10.1039/b000000x

Abstract

Optimization of various process parameters for development of poly (lactic-co-glycolic acid, PLGA) coating on Mg-Al layered double hydroxide (LDH) nanoparticles intercalated with anticancer drug methotrexate (MTX), is reported here. Both double and single emulsion-solvent evaporation techniques were adapted to synthesize the PLGA coated, MTX drug loaded nanoparticles as above, with and without LDH. While keeping some of the process parameters constant , the homogenization speed, concentration of PLGA, LDH-MTX, MTX and surfactants, aqueous and organic phase volume involved in the synthesis of the PLGA-MTX and PLGA-LDH-MTX nanoparticles as above, were varied and evaluated to obtain the desired particle size range and drug entrapment efficiency for specific use. The optimized and a few selected unoptimized nanoparticles as above in turn were further assessed for *in vitro* drug release kinetics and time and dose dependent *in vitro* cell viability bioassay, *in vitro* MTX uptake study using human osteosarcoma, MG-63 cell line. The *in vivo* pharmacokinetic study exhibited much higher therapeutic efficacy of the optimized PLGA-LDH-MTX and PLGA-MTX nanoparticles in terms of enhanced half life of the drug and slow clearance rate compared to the bare MTX drug.

Keywords: Optimization of process parameters, Mg-Al layered double hydroxide, double and single emulsion solvent evaporation technique, drug entrapment efficiency, poly (D, L-lactide-coglycolide) coating, methotrexate drug.

Introduction

Osteosarcoma is an aggressive malignant neoplasm among all age groups, particularly in adolescence.[1] Every year, more than thousand new cases are diagnosed and reported worldwide.[2,3] The 5 year survival rate for the patient diagnosed with osteosarcoma is only about 10%. This dismal scenario is due to the fact that initially, the cancer is often asymptomatic, hence is not detected until the advanced stages .[4-6] Various treatment options, e.g., chemotherapy, radiation therapy, hormonal and targeted therapy have been used to treat the different stages of osteosarcoma, although, chemotherapy continues to be the major therapeutic opinion for patients with metastatic bone cancer.[7,8] Hence, importantly, the chemotherapeutic agents must be able to kill or inhibit growth of neoplastic cells, selectively, leaving the normal cells unharmed. However, most of the currently available drugs used for bone cancer, tend to damage the DNA (deoxyribose nucleic acid) or DNA synthesis, killing all rapidly dividing cells, both normal and cancerous.[9-11] Lack of target selectivity is a major problem here, additionally, most patients develop drug resistance or refractory disease in this status, eventually requiring second-line therapy.[12,13] Recently, the American cancer society recommended high dose methotrexate (HDMTX) in multi agent combination with folinic acid rescue to provide relapse-free survival rates, to the extent of >50% and as a result, became central to modern chemotherapy regimen for bone cancer.[14,15] However, the major hindrance for use of methotrexate as chemotherapeutic agent is its poor solubility, poor bio availability and narrow therapeutic index, characteristic of a BCS (biopharmaceutics classification system) class IV drug in general. Furthermore, prompt recognition and treatment of methotrexate (MTX)-induced renal dysfunction are essential to prevent potentially life-threatening MTX-associated toxicities, especially myelosuppression, mucositis, and dermatitis.[16-18]

In view of the above, despite the versatility of methotrexate as a chemodrug in general and for specific use in osteosarcoma, it is difficult to be used in the first-line therapy, either as a single agent or in combination with other anticancer drugs. In this regard, the current research worldwide on novel nanoformulations of the existing chemodrugs to improve their therapeutic efficacy paves the possibility to overcome the intrinsic problems of the BCS (biopharmaceutics classification system) class IV anticancer drug methotrexate for the said use. Over the last decade, extensive research on carrier mediated drug delivery systems using liposomes, dendrimers, water soluble polymer and polymer-protein conjugates has catered to some potent chemotherapy agents, e.g., abraxane, doxil etc.[19-24] that takes care of the intrinsic problems of the chemodrugs as above, and exhibit much higher therapeutic efficacy compared to their bare drug counterparts.

Although drug delivery is a polymer dominated field, the search of an alternative inexpensive and broad spectrum material has undoubtedly arrived at nanophase ceramics that has been in biomedical application since ages.[25, 26] In the fastest emerging area of drug delivery, their extraordinary characteristics, e.g., size, highly active surfaces, ease of modification, structural advantages, tailor made physical and chemical properties suggest that they can be excellent platform for drug transportation and controlled release analogous to their polymeric counterparts.[27, 28] Pertinent to the area, the nanoparticles of layered double hydroxide, a class of anionic clay have attracted much attention as the new age drug delivery vehicle because of their biodegradability, biocompatibility and tailor made anion exchange behavior and non toxicity.[29-32] Broadly, it comprises cationic bi layers and charge balancing anions in the interlayer space, represented by the general formula $[M(II)_{(1-x)}\ M(III)_{x}\ (OH)_2]\ [A^{n-}]_{x/n} \cdot m\ H_2O$, where M(II) is a divalent and M(III) is a trivalent cation, A^{n-} is a gallery anion, x is equal to the ratio M(III)/[M(II)+M(III)], and m is the number of moles of co-intercalated water per formula weight of the compound.[33-36] In our earlier work we have already reported the possibility of the coating of methotrexate (MTX) loaded LDH (layered double hydroxide) vehicle (LDH-MTX nanohybrid) using an anionic, hydrophobic polymer, PLGA, that might help to improve the overall therapeutic efficacy of methotrexate while reducing its inherent toxicity, indicating possibility of its use as a first line chemotherapeutic agent for treatment of osteosarcoma.[37]

In continuation, in the present communication we report the optimization of the process parameters for the fabrication of PLGA [poly (lactic-co-glycolic acid)] coated LDH-MTX (layered double hydroxide-methotrexate) nanohybrid to improve the therapeutic efficacy of the BCS (biopharmaceutics classification system) class IV drug methotrexate, in terms of improved bioavailability, pharmacokinetic/*in vitro* release profile, reduced toxicity etc., analogous to the characteristics of first line therapy chemodrugs. To obtain the above, we primarily made an attempt to evaluate various processing and formulation parameters, e.g., homogenization speed, concentration of PLGA, LDH-MTX, MTX and surfactants, aqueous and organic phase volume etc. that might affect the characteristics of the final dosage form of the optimized PLGA-MTX and PLGA-LDH-MTX nanoformulations. Hence, the whole procedure of optimization helps in validation of the preparative conditions of the said dosage form from bench scale to pilot scale, to attain our desired target. The optimized nanoparticles as above have been characterized using infrared spectrophotometry, scanning and transmission electron microscopy, dynamic laser scattering and thermal analyses. The drug loading and *in vitro* release studies have been carried out in PBS (phosphate buffered saline) medium at pH 7.4, using high performance liquid chromatography (HPLC). The time and dose dependent cell viability assay using human osteosarcoma cell line (MG-63) of the optimized PLGA coated MTX and LDH-MTX exhibited higher efficacy compared to pure MTX drug, (active pharmaceutical ingredient, API) in the time periods of 48, 72 and 96 h, while the pharmacokinetic (healthy) study using New zealand white rabbit model reveals an enhanced elimination half life ($t_{1/2}$) of the drug, with much slower clearance rate and longer retention time of optimized formulation, compared to its bare MTX counterpart.

Experimental section

Materials

Methotrexate (molecular weight, 454.50 g/mol) was obtained as a gift sample from M/s Naprod Life Sciences, Mumbai, India. Magnesium nitrate hexahydrate, Mg $(NO_3)_2.6H_2O$, aluminum nitrate nonahydrate, Al $(NO_3)_3.9H_2O$, sodium hydroxide, NaOH and ammonium acetate, CH_3COONH_4 were purchased from M/s Sigma Aldrich, Bangalore, India. The polymer, poly (D, L–lactide-coglycolide) (PLGA), with a copolymer ratio of D, L-lactide to glycolide of 50:50 (molecular weight in the range, 24,000-38,000 g/mol) was purchased from M/s Boehringer Ingelheim Pharma Gmbh & Co., Germany. The non ionic surfactant and emulsifier Sorbitane Monooleate (Span 80), Polyoxyethylene sorbitane monooleate (Tween 80) and poly (vinyl alcohol, PVA, (water soluble, 87-90% hydrolysed, molecular weight 30,000-70,000) were purchased from M/s Merck Specialties Pvt Ltd, Mumbai, India. The solvent dichloromethane (DCM), acetone and other chemicals of AR grade were purchased from M/S Sigma Aldrich, St. Louis, MO, USA. Deionised and decarbonated ultrapure water (Millipore, specific resistivity 18.2 MΩ) was used in all the syntheses as above and the chemicals utilized in this study were used as received without further purification. The nitrogen gas used for synthesis and characterization in the present work was of XL grade having the percentage purity, 99.999%.

Preparation of pristine LDH

The simple co- precipitation technique that was adapted here has been reported in details in our earlier work.[38-40] In brief, an appropriate volume of NaOH (0.5M) was added drop wise, under a nitrogen atmosphere (XL grade, % purity, 99.999 %) to a solution containing Mg $(NO_3)_2 \cdot 6H_2O$ (0.64 mol) and Al $(NO_3)_3 \cdot 9H_2O$ (0.32 mol) in 250 ml of ultra-pure (Millipore, specific resistivity 18.2M Ω) decarbonated water (Mg/Al = 2.0), reaching a pH of about 11.0±0.5. The resulting slurry was stirred vigorously, stirred in magnetic stirrer (@1100 rpm, IKA C-MAG HS7, Germany) and aged at 25±3 ºC for 24 h .The resulting samples were then centrifuged for (Heal Force, Neofuge 15R, China) 10 min at 8519 g rcf, washed three to four times with decarbonated ultra-pure water and dried at freeze drier (EYEL4, FDU2200, Japan) at -82 ºC and 20 Pa pressure for 12h, to get LDH.

Intercalation of methotrexate in pristine LDH

The intercalation of methotrexate drug into LDH bilayer was carried out by an *ex-situ* anion exchange method. In this method, the drug solution was prepared by addition of 1.00 gm of MTX in 100 ml of (0.3 M) ammonium acetate solution, to attain resulting pH to be ~ 7.00. The above solution was then added drop wise to a 1% (w/v) aqueous suspension of pristine LDH and was continued at 25±3 ºC for a period of 48 h in a constant temperature bath. It was then centrifuged at 8519 g rcf (Heal Force, Neofuge 15R, China), washed three to four times with decarbonated water, and dried in a freeze drier as above to get LDH-MTX nanohybrid[37,41] (Scheme 1).

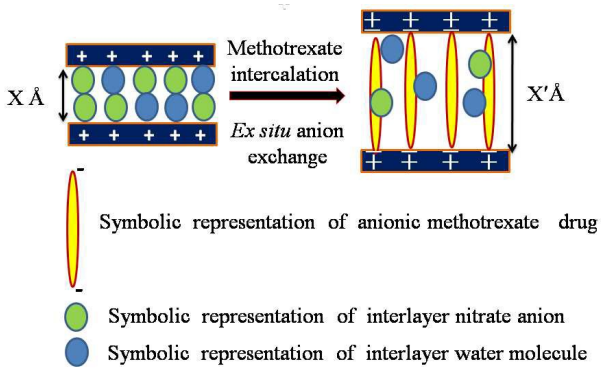

Scheme 1 Intercalation of MTX drug within the interlayer space of LDH.

Optimized method for synthesis of PLGA-LDH-MTX nanoparticle by double emulsion ($W_1/O/W_2$)-solvent evaporation method

In this method, LDH-MTX in lyophilized powder form (equivalent to 100 mg of MTX present in LDH-MTX, loading calculated by HPLC analysis) was added to 5 ml of decarbonated water and sonicated for 5 min to get a homogeneous suspension of LDH-MTX naoparticles in aqueous medium. The suspension was added drop wise through a 16 gauge needle syringe at a flow rate

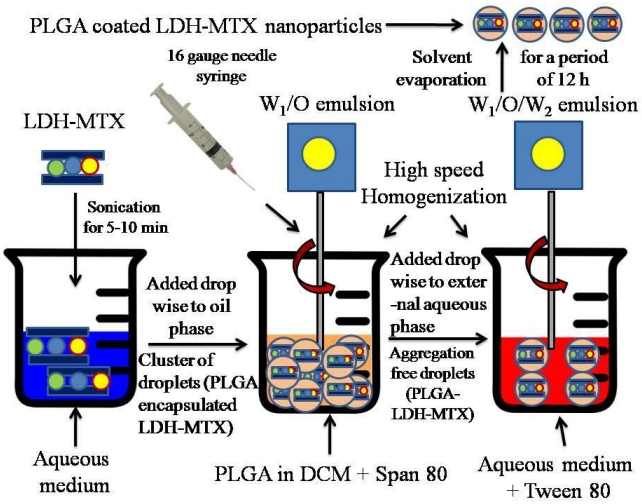

Scheme 2 Optimized technique for synthesis of PLGA-LDH- MTX nanoparticle by $W_1/O/W_2$ double emulsion- solvent evaporation method.

of 3 ml /min (approximately) in 10 ml of organic phase (DCM, Dichloromethane) containing a weighed amount of PLGA (LDH-MTX: PLGA in 1:2 ratio by weight) and span 80 as surfactant (span 80, 0.5% w/v) under high speed homogenization at speed of 12000 rpm (IKA T25 ULTRA-TURRAX®, Germany) for 5 min, to get a primary emulsion (W_1/O). The resulting water-in-oil (W_1/O) emulsion was further added drop wise into 20 ml of an aqueous solution of 2% (w/v) tween 80 (W_2) used as an emulsion stabilizer to minimize coalescence of the emulsion and aggregation of the particles formed. The mixture was further homogenized for 5 min @ 12,500 rpm to obtain a double $W_1/O/W_2$ emulsion. The organic solvent (DCM) was allowed to evaporate slowly for a period of 12 h at room temperature under agitation (@500 rpm) using a magnetic stirrer (IKA C-MAG HS7, Germany) (Scheme 2). Consequently the polymer, insoluble in the aqueous phase, precipitated as solid particles, on encapsulation of the LDH-MTX nanohybrid. The resulting sample was collected by centrifugation @ 8519 g rcf (Heal Force, Neofuge 15R, China), for 25 min and washed thrice with deionised water to remove the excess surfactant and uncoated LDH-MTX.[37,42,43] The resultant PLGA-LDH-MTX nanoparticle was freeze-dried to obtain a fine powder. Each sample was prepared in triplicate to check reproducibility of the process.

Optimized method for synthesis of PLGA-MTX nanoparticles by single emulsion (O/W) -solvent evaporation method

Briefly, 500 mg of PLGA and 250 mg MTX (2:1 by weight) were dissolved in 10 ml of acetone, and then added drop wise through a 16 gauge needle syringe to 15 ml of a 2% (w/v) poly (vinyl alcohol) aqueous solution. The emulsion thus formed was homogenized (@ 12000 rpm) using a high speed homogenizer for 5 min and was stirred for a period of 12 h for complete evaporation of the solvent, acetone, to precipitate the PLGA encapsulated MTX nanoparticles (Scheme 3).

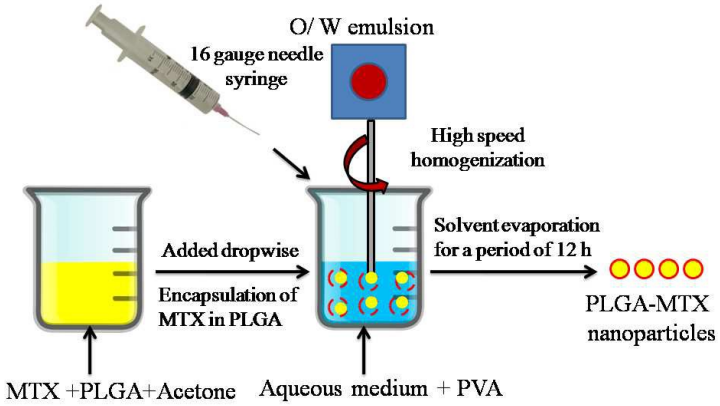

Scheme 3 Development of PLGA-MTX nanoparticle by O/W single emulsification-solvent evaporation method.

The resulting sample was collected by centrifugation at 8519 g rcf for 10 min and was washed several times with decarbonated water to remove the residual nonionic surfactant, PVA. Finally, the particles were resuspended in a cryoprotectant (1% w/v mannitol solution) and freeze dried at-82 ºC with a vacuum pressure of 20 Pa. Each sample was prepared in triplicate to check reproducibility of the process.[44, 45]
The methods elaborated as above are optimized, w.r.t all the synthesis and processing parameters.

Drug entrapment efficiency of optimized batches of PLGA-LDH-MTX and PLGA-MTX nanoparticles

Both the freeze dried (~100 mg by weight) PLGA-LDH-MTX and PLGA-MTX nanoparticles prepared as above were added in 10 ml of acetone to dissolve the polymer and the drug was extracted in phosphate buffer saline solution at pH 7.4. The resulting solution was then centrifuged at 2739 g rcf for a period of 5 min and the supernatant was filtered through membrane filter (0.22 µm, Merck-Millipore, USA) and analyzed by HPLC method to determine the drug entrapment efficiency of both the nanoparticles as above (see eqn (S1), (S2) and (S3) in ESI).[37,46]
All experiments were carried out in triplicate and the errors were expressed as SD.

Determination of residual surfactant PVA in the optimized batch of PLGA-MTX nanoparticles

Although PVA is a widely used polymeric surfactant in the external aqueous phase as an emulsifier, the safety of PVA still appears to be a concern from the previous literature reports. [47] Following repeated subcutaneous or intravenous administrations of PVA, various organ lesions and hypertension have been reported in rats, central nervous system depression and anemia followed by renal damage have also been reported in beagle dogs. Therefore, residual PVA present, if any, needs to be estimated and then removed by washing procedures such as repetitive centrifugation or filtration. In the present case, the residual amount of the surfactant PVA was determined by colorimetric method, resulting in formation of a colored complex. In brief, 5 mg of lyophilized powder of PLGA-MTX nanoparticles was taken and treated with 5 ml of 0.5 M sodium hydroxide solution for 15 min at 60ºC. Then the sample was neutralized with 2 ml of 1N HCl and finally, the volume was made up to 10 ml with distilled water. To this, 5 ml of 0.65 M aqueous solution of boric acid, 1.25 ml of potassium iodide (0.15 M) and 2 ml of water was added. Finally the solution was incubated for 10 min and the absorbance was measured at 690 nm.[48,49] The above was repeated in triplicate and finally, the amount of residual PVA was determined from the standard curve (see Fig. S1 in ESI).

***In vitro* release study of MTX from the optimized PLGA-MTX, PLGA-LDH-MTX and unoptimized [PLGA-MTX (L) and (H) and PLGA-LDH-MTX (L) and (H)] nanoparticles**

In vitro release of MTX from the optimized batches of PLGA-LDH-MTX and PLGA-MTX nanoparticles were carried out using type-II USP dissolution test apparatus (Electrolab TDT-146 08L Mumbai, India). In this, 0.1g (drug entrapment efficiency of PLGA-LDH-MTX is 65%) of PLGA-LDH-MTX and 0.075 g PLGA-MTX nanoparticles (drug entrapment efficiency of PLGA-MTX is 35%) were placed in a dialysis tubing cellulose membrane bag (cut off molecular weight 14 KD, M/s Sigma-Aldrich, St. Louis, MO 63178 USA) separately and immersed in 900 ml of PBS (pH 7.4) maintained at 37.2 °C with constant stirring @ 100 rpm. At specific time intervals, 10 ml of aliquot was withdrawn and replenished with same volume of the medium immediately, followed by analysis of the aliquot as per standard procedure.[37] *In vitro* drug release study of the unoptimized nanoparticles were carried out using, 0.170 gm of PLGA-MTX (L) (drug entrapment efficiency, 15.84%), 0.040 gm of PLGA-MTX (H) (drug entrapment efficiency, 62.28%), 0.570 gm of PLGA-LDH-MTX (L) (drug entrapment efficiency, 4.39%) and 0.0284 gm of PLGA-LDH-MTX (H) (drug entrapment efficiency, 89.96%) nanoparticles, following the same procedure as above.

***In vitro* bioassay**

Cell culture

MG-63 human osteosarcoma cells were obtained from ATCC (Rockville, MD, USA), cultured in the DMEM (Invitrogen, Carlsbad, USA) growth medium supplemented with 10% foetal bovine serum (Gibco, Invitrogen, UK), 2 mg ml^{-1} sodium bicarbonate and 1% (10 ml in 1000 ml medium) penicillin- streptomycin (Sigma Aldrich, Bangalore, India). The cells were grown at 37ºC in a humidified 5% CO_2 (HF90 Heal Force, China) incubator. The cells were sub-cultured using trypsin–EDTA when they were 90–95% confluent.[41,50] All the experiments were done with the cells when they were within ten passages after revival from cryopreservation.

Time and dose dependent cell viability assay of the optimized PLGA-MTX, PLGA-LDH-MTX and unoptimized [PLGA-MTX (L) and (H) and PLGA-LDH-MTX (L) and (H)] nanoparticles on MG-63 cell line

The dose dependent efficacy of pure MTX (active pharmaceutical ingredient, API) drug and the optimized PLGA-LDH-MTX and PLGA-MTX nanoparticles on the viability of MG-63 (Human osteosarcoma) cell line were determined by MTT assay at four different time points of 24, 48, 72 and 96 h. The selected concentrations for the above dosage were 25, 50, 75 and 100 µg/ml, respectively, taking into account from lower to higher range. Briefly, 3×10^4 of MG-63 cells per ml were plated in 96 well microtiter plates in triplicate and incubated in 5% CO_2 incubator for 24 h. Then, 200 μl of freshly prepared concentrations (25, 50, 75 and 100 µg/ml) of pure drug MTX, PLGA-LDH-MTX and PLGA-MTX nanoparticles containing the same amount of

drug concentration as above, was added to the wells as above and was further incubated for 24, 48, 72 and 96 h under the same conditions. To estimate the cell viability, at each time point, the plate was removed and treated with 100 μl of MTT(3-[4, 5-dimethylthiazol- 2-yl]-2, 5-diphenyltetrazolium bromide, Sigma-Aldrich, USA) solution (2 mg ml^{-1} in PBS) was added to each well and incubated for 4 h. Next, MTT was gently replaced by 100 μl dimethyl sulphoxide (DMSO) to dissolve formazan crystals and the absorbance was measured using a plate reader (Bio-Rad, USA), at 550 nm to determine the percentage cell viability,[51] to estimate the dose dependent efficacy at the time points as above. The same procedure as above has been carried out for the unoptimized [PLGA-MTX (L) and (H) and PLGA-LDH-MTX (L) and (H)] nanoparticles, as well.

***In vitro* study of MTX uptake using both optimized PLGA-MTX, PLGA-LDH-MTX and unoptimized [PLGA-MTX (L) and (H) and PLGA-LDH-MTX (L) and (H)] nanoparticles on MG-63 cell line**

In vitro cellular uptake study was performed using human osteosarcoma cancer cell line (MG-63).[52,53] The method in brief, 6 well plates were seeded with 1×10^6 cells per well and incubated in DMEM medium at 37°C in humidified atmosphere containing 5% CO_2 for 24 h to attach the cells. After 24 h the medium of each well was replaced with 3 ml of suspension comprising optimized PLGA-MTX, PLGA-LDH-MTX and unoptimized [PLGA-MTX (L) and (H) and PLGA-LDH-MTX (L) and (H)]nanoparticles (1500 µg/well) and incubated further for 6, 15 and 24 h, respectively. At each time points the cells were then washed with PBS (phosphate buffered saline) to remove the nanoparticles which were not internalized. Next, the cells were lysed by incubating them with 0.5 ml of RIPA lysis buffer system (RIPA Buffer, Sigma, R0278) for 10 min at 4°C in ice cold water. A 500 µl of each cell lysate aliquot was used immediately for the cell protein determination and the remaining portion was centrifuged at 8519 g rcf (Heal Force, Neofuge 15R, China) for 5 min at 4°C to pellet the cell debris. Finally, the supernatant was collected and analyzed for MTX drug by a high performance liquid chromatography (HPLC) method described previously.[37] The concentration of the drug, methotrexate was determined from the chromatograms (based on the standard calibration curve of MTX) and corresponding to the same, the amount of drug uptake in the cells, w.r.t the time points have been plotted.

***In vivo* pharmacokinetic studies**

The *in vivo* pharmacokinetic studies to estimate the salient pharmacokinetic parameters, e.g., area under curve, elimination half life, volume of distribution, elimination rate constant and clearance rate were carried out in healthy New Zealand White (NZW) variety of rabbits (*Oryctolagus cuniculus*) of either sex weighing approximately 1.60-1.80 kg, aged, 10-12 months.[54] The experiment/study protocol was approved by the Institutional Ethical Committee, West Bengal University of Animal and Fishery Sciences, Kolkata, India. The animals were fed with rabbit pellet diet, formulated feed (EPIC, Govt. of West Bengal), grams and green vegetables and provided with water, *ad libitum*. The temperature of the animal room was maintained at 22 ± 3°C and provided with 12 h day night artificial lighting facilities. The animals were divided into three groups (n = 6), each of the three groups were injected with bare MTX, optimized PLGA-MTX and PLGA-LDH-MTX nanoparticle at an equivalent dose of 15 mg/kg of body weight. The blood samples were collected from right marginal ear vein of all animals of three groups into heparinated tubes at 0 h (pre-drug administration), 0.08 h upto 240 h at different time intervals of post dosing and the blood samples were immediately centrifuged (Remi Equipments Ltd., Mumbai, India) at 2739 g rcf, for 20 min and the plasma was stored at -20 ºC for further drug analysis. Protein precipitation was performed prior to HPLC analysis. Briefly, 500 µL blood plasma sample was mixed with 100 µl of a solution of trichloro acetic acid in ethanol and extracted on a vortex mixer (MixMate, Eppendorf, USA) for 2 min, then placed on ice bath for 15 min to enhance protein precipitation.[55] The samples were centrifuged at 986 g rcf for 15 min and filtered through 0.22 µm membrane filter. Finally, 20 µL of the filtered sample was injected into the HPLC column (C18, XBridge, 150×4.6 mm, Waters, USA) for analysis.

Instruments and characterization

Particle morphology and size of the PLGA-LDH-MTX and PLGA-MTX nanoparticles were examined by a Carl Zeiss SMT AG SUPRA 35VP (Germany) field emission scanning electron microscope (FESEM). The elemental composition of the samples (data not shown here) was studied using energy dispersive X-ray spectroscopy (EDX) attached to the FESEM. Particle size, polydispersity index (PDI) and zeta potential were measured using a Zetasizer Nano ZS (M/s Malvern, Worcs, UK) based on quasi-elastic light scattering. The samples were dispersed in deionized water and diluted 1/5 (v/v) with the same at room temperature. Zeta potential was measured using the same instrument at 25 ºC following a 1/10 (v/v) dilution in deionised water.
All the experiments as above were repeated at least three times to check the reproducibility of the results. Fourier–transform infrared spectra (FTIR) were recorded in a spectrophotometer (Perkin–Elmer Frontier™ IR/FIR**,** Waltham, USA) using KBr (M/s Sigma Aldrich, > 99% pure) pellet (sample: KBr 1:100 by weight) spectrometer in the 400–4000 cm^{-1} range with average of 50 scans to improve the signal to noise ratio. The physical compatibility of MTX drug entrapped in the sample PLGA-LDH-MTX and PLGA-MTX was determined by the differential scanning calorimetry (STA 449 F3 Jupiter®, NETZSCH, Germany). In this, ~5 mg of MTX,LDH, LDH-MTX,PLGA, PLGA-LDH-MTX,PLGA-MTX, physical mixture of MTX and PLGA, and (MTX: LDH in 1:1 ratio by weight as placebo nanoparticles were sealed in standard aluminum pans with lids and were heated from ambient to 500ºC (@ 5 ºC/min) in nitrogen atmosphere. Particle size, morphology and crystallographic analyses of PLGA-MTX and PLGA-LDH-MTX nanoparticles were studied using transmission electron microscopy (FEI Tecnai F30 G^2 S-Twin, The Netherlands) operated at 300 kV. Grid for TEM study was prepared by dropping a micro droplet of suspension of LDH powder in isopropyl alcohol on to a 400 mesh carbon-coated copper grid and drying the excess solvent naturally. Microanalysis of the samples (elemental composition) were performed using energy dispersive spectroscopy (EDS) with a low system back ground

(<1% spurious peaks), high P/B ratio (Fiori number >4000) having spectrum imaging with Si–Li detector attached to the TEM equipment.

Results and discussion

Effect of process parameters on PLGA-MTX and PLGA-LDH-MTX formulation characteristics

The effect of the process parameters such as homogenization speed, concentration of PLGA, LDH-MTX, MTX and surfactants, aqueous and organic phase volume involved in the synthesis of the PLGA-MTX and PLGA-LDH-MTX nanoparticles either by single or double emulsion-solvent evaporation techniques were evaluated to achieve their desired particle size range and drug entrapment efficiency for specific use.

Effect of homogenization speed on drug entrapment efficiency and particle size

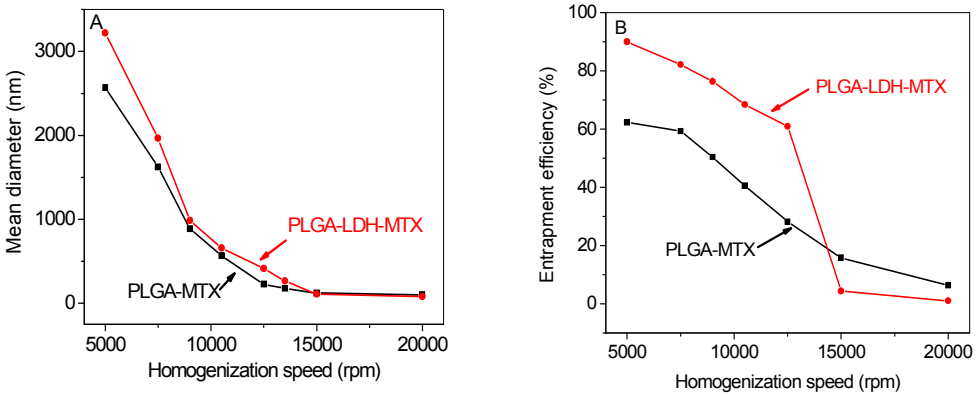

Fig. 1 Effect of homogenization speed on (A) Particle size (mean diameter) (B) Percentage of drug entrapment efficiency of PLGA-MTX and PLGA-LDH-MTX nanoparticles.

The homogenization speed during the preparation of the primary emulsion was varied from 5000 rpm to 20,000 rpm while the homogenization speed of the secondary emulsion was constant, and the effect of variation in homogenization speed on particle size is shown in Fig.1, panel A. The increase in speed as above from 5000 to 20,000 rpm rendered a concomitant increase in breaking energy, resulting in smaller emulsion droplets and thus a narrow particle size distribution for both PLGA-MTX and PLGA-LDH-MTX nanoparticles as above.[56,57] Fig.1, panel B shows the effect of homogenization speed on the drug entrapment efficiency of PLGA-MTX and PLGA-LDH-MTX nanoparticles. The entrapment efficiency of PLGA coated MTX nanoparticles was found to be 60 % at 5000 rpm that decreased to 15.84% at 15000 rpm. At lower speed, the higher particle size exhibits higher entrapment efficiency on account of lower surface area that leads to less transport of the methotrexate into the external aqueous phase, while at a higher homogenization speed, comparatively lower particle size comprises much higher surface area that renders faster transport of the entrapped drug as above from the dispersed organic phase to the continuous aqueous phase.[57, 58] On the other hand, the entrapment efficiency of PLGA coated LDH-MTX nanoparticles was 89.96% at 5000 rpm and only 4.39% at 15,000 rpm. The marked decrease in entrapment efficiency of PLGA-LDH-MTX may be attributed to the exfoliation of the lamellar structure of the LDH in LDH-MTX, while being encapsulated in PLGA polymer in the primary emulsion, possibly. This resulted in fast escape of MTX drug from the inter layer space of LDH-MTX, leading to a substantial decrease in loading.

Effect of PLGA concentration of the internal organic phase (DCM/Acetone) on drug entrapment efficiency and particle size

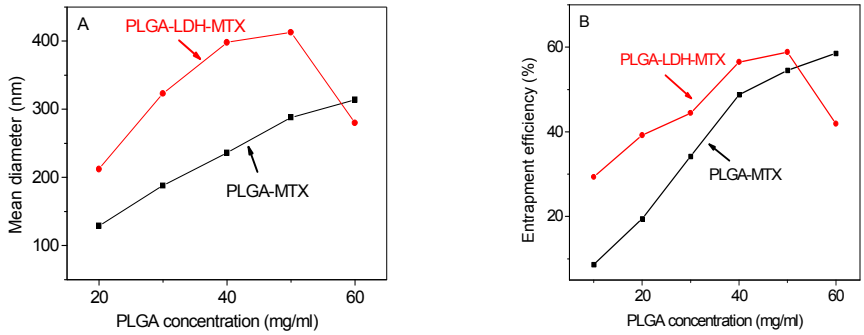

Fig. 2 Effect of polymer (PLGA) concentration on the (A) Particle size and (B) Percentage of drug entrapment efficiency of PLGA-MTX and PLGA-LDH-MTX nanoparticles.

Fig. 2, panel A shows the effect of PLGA concentration in the organic phase on the mean diameter of the above two batches of nanoparticles produced by homogenization. The polymer (PLGA here) concentration was varied from 20 to 60 mg ml^{-1} for the PLGA coated nanoparticles, while keeping other processing parameters constant. The increase in the PLGA concentration leads to a gradual increase in the nanoparticle diameter for both (PLGA-MTX and PLGA-LDH-MTX), with a broad size distribution. This might be attributed to the enhanced viscosity of the organic phase in both the cases, resulting in resistance against shear forces during the emulsification and inappropriate dispersability of organic phase into the aqueous phase,[59] until a limit concentration of 50 mg ml^{-1}. Beyond this, in case of PLGA-LDH-MTX, despite the high speed homogenization (constant at 15000 rpm) being continued, the substantial increase in viscosity at a concentration > 50 mg ml^{-1} for PLGA in the primary emulsion, possibly hinders the coating process on the LDH-MTX nanoparticles. Hence, the incompletely coated PLGA-LDH-MTX nanoparticles exhibit a sudden drop in the mean diameter of the same.
Drug entrapment efficiency of both the nanoparticles as above, increased with increase in the polymer concentration upto a certain limit, in the organic phase (Fig. 2, panel B). Increase in the amount of polymer increase the viscosity of organic phase that, in turn, renders hindrance to drug diffusion from organic to aqueous phase.[59,60] In case of PLGA coated MTX nanoparticles, it might be possible that increase in polymer concentration increased the diameter of the nanoparticles, and thereby increased the diffusional pathway of drug into the aqueous phase, reducing the drug loss through diffusion and increasing the drug content.[61,62] In case of PLGA coated LDH-MTX, it was observed that initial increase of entrapment efficiency followed by a marked decrease, on account of substantial variation in particle size as demonstrated above (Fig. 2, panel A). In addition to this, considering the thermodynamic stability of the system, marked by balancing a number of molecular interactive forces at the interface of the hydrophilic LDH core intercalated with the hydrophobic methotrexate drug, encapsulated altogether in the hydrophobic PLGA shell is achieved until a limit concentration, beyond which, the physical phenomenon of polymer chain loosening starts, indicating a possibility of drug loss and thereby reduction of the entrapment efficiency as shown in Fig. 2, panel B. See Table S1 in ESI for detail information about the related parameters.

Effect of surfactant concentration (span 80) of the internal organic phase (DCM) on drug entrapment efficiency and particle size for development of PLGA-LDH-MTX nanoparticles

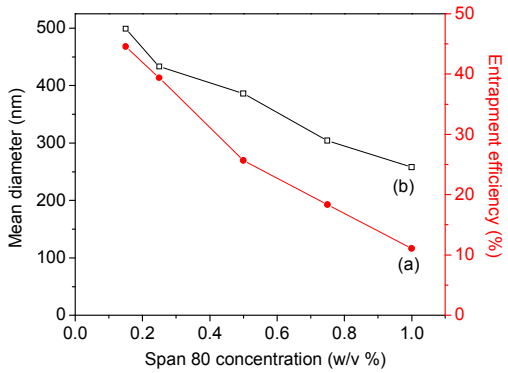

Fig. 3 Effect of surfactant concentration (span 80) on the (a) Particle size and (b) Percentage of drug entrapment efficiency of PLGA-LDH-MTX nanoparticles.

To improve the physical stability of the primary emulsion as well as to prevent the aggregation of the nanoparticles, span 80 was added to the organic phase at a range of concentration of 0.15 to 1.0% (w/v). Based on the unsaturated branched chain fatty acid (sorbitan monoleate) span 80 is an effective lipophilic surfactant with a moderate HLB value of 4.3, it aids to minimize the interfacial tension of the W_1/O primary emulsion leading to formation of aggregation free, polymer encapsulated nanoparticles of PLGA-LDH-MTX, as shown in Fig. 3 (b). This stabilizes the smaller droplets of the system, resulting in the formation of narrow size distribution of the PLGA coated LDH-MTX nanoparticles. However, the highly surface active nanoparticles of smaller size herewith render a substantial drug loss during washing, compared to the larger ones, exhibiting a decreasing trend of drug entrapment efficiency with increasing surfactant concentration as above.[63]

Effect of surfactant concentration (PVA/Tween 80) of the external aqueous phase on drug entrapment efficiency and particle size

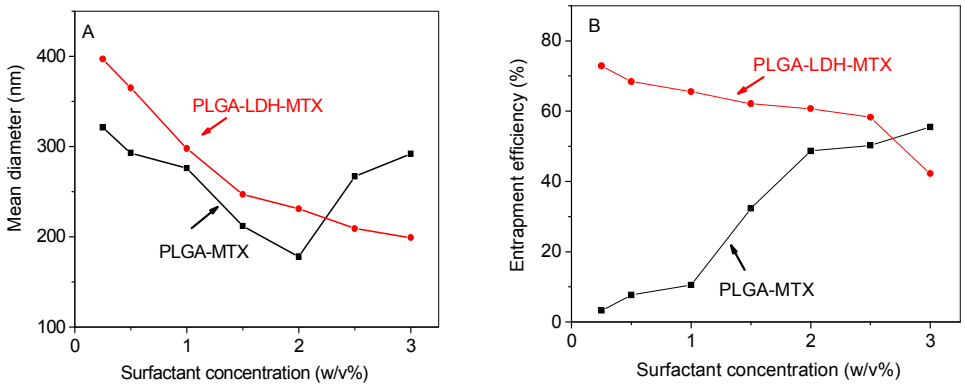

Fig. 4 Effect of the surfactant concentration (PVA, Tween 80) on (A) Particle size distribution. (B) Percentage of drug entrapment efficiency.

The concentration and type of surfactant, which plays an important role to protect the dispersed droplets from coalescence, stabilizes an emulsion. In the present study two different types of emulsification methods have been used to encapsulate the bare drug MTX and the LDH-MTX nanoparticles within PLGA polymer. To know the influence of surfactant content on the nanoparticle properties, same batches were prepared using different concentrations of non ionic surfactants PVA and tween 80 in an external aqueous phase. With regard to particle size, a linear pattern of reduction could be obtained in case of PLGA-LDH-MTX nanoparticles, on account of an optimum interfacial stabilization by the hydrophilic surfactant tween 80 with a high HLB value of 15 (Fig. 4, panel A). On the contrary, for PLGA-MTX, PVA has been used as surfactant in the external aqueous phase and an increase in the surfactant concentration here decrease the size of the nanoparticles on account of an enhanced interface stabilization upto a certain extent, beyond which, increased viscosity of the medium reduces the net shear stress available for the droplet break down, leading to increase in the particle size (Fig. 4, panel A).[59,64]
With regard to drug entrapment efficiency, in case of PLGA-MTX, (Fig. 4, panel B) an optimum concentration of PVA tends to reduce the particle size as above and is thereby associated with larger surface area of the nanoparticles that enhances the possibility of the drug molecules to be attached to the nanoparticle surfaces, leading to higher drug entrapment efficiency.[65] On the contrary, for PLGA-LDH-MTX, (Fig. 4, panel B) an enhanced concentration of tween 80 in the external aqueous phase aids in reduction of entrapment efficiency of the nanoparticles on account of the hydrophilic LDH core of the PLGA coated surface active particles that aids in slow diffusion of the MTX drug in the external aqueous phase, leading to a linear pattern of decrease in entrapment efficiency.[66] See Table S2 in ESI for detail information about the related parameters.

Effect of volume of organic and aqueous phase on drug entrapment efficiency and particle size

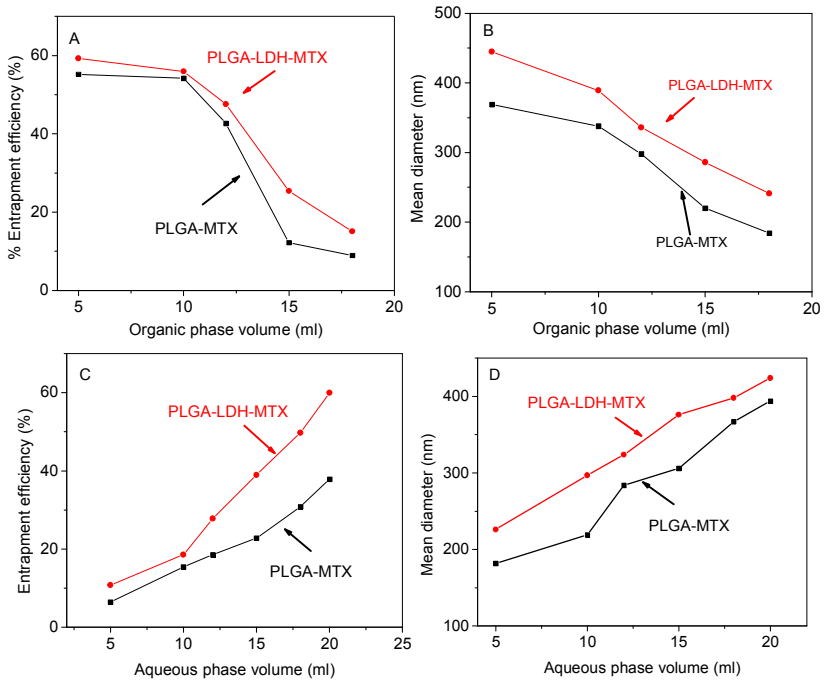

Fig. 5 Effect of volume of organic and aqueous phase on (A), (C) Percentage of drug entrapment efficiency and (B), (D) Particle size of PLGA-MTX and PLGA-LDH-MTX nanoparticles.

In the present study we explore the effect of the volume of organic phase on the drug entrapment efficiency of two different nanoparticles e.g. PLGA-MTX and PLGA-LDH-MTX. Fig. 5, panel A shows that the entrapment efficiency decreased with increasing volume of organic solvent, e.g., dichloromethane for PLGA-LDH-MTX and acetone for PLGA-MTX. This is due to the decreased viscosity of the drug-polymer solution in the organic phase of the primary emulsion, resulting in faster diffusion of the drug into the external aqueous phase, lowering the drug entrapment efficiency, in both the cases as above.[59,67] Fig. 5, panel B shows decrease of particle size with the increasing of volume of organic phase. This can be explained that increase of solvent volume lowering the viscosity of polymer concentration in organic phase, resulting decrease in resistance against shear forces during the emulsification, resulting smaller droplet formation. Hence, formation of smaller size nanoparticles.[59]
Fig. 5, panel C shows that as the aqueous phase volume increased entrapment efficiency also increased for both of the nanoparticles PLGA-MTX and PLGA coated LDH-MTX produced by homogenization.[59,68] It is clearly observed that increasing aqueous volume result in an increase Of drug entrapment efficiency; it could be due to lesser aggregation of the particles in a larger volume.[69] This condition aids in faster solidification of the polymer present in the organic phase, across the phase boundary, leading to an increased particle size and thereby, higher drug entrapment efficiency.
With regard to mean diameter, Fig. 5, panel D shows an increasing trend of the same for PLGA-LDH-MTX and PLGA-MTX both, with increasing external aqueous phase volume. A probable explanation is that with increasing the external volume, the shear forces to break the emulsion droplets become smaller yielding larger emulsified droplets which in turn results in larger PLGA nanoparticles.[59- 60,69]

Effect of MTX concentration of the organic phase and LDH-MTX concentration of the aqueous phase on drug entrapment efficiency and particle size

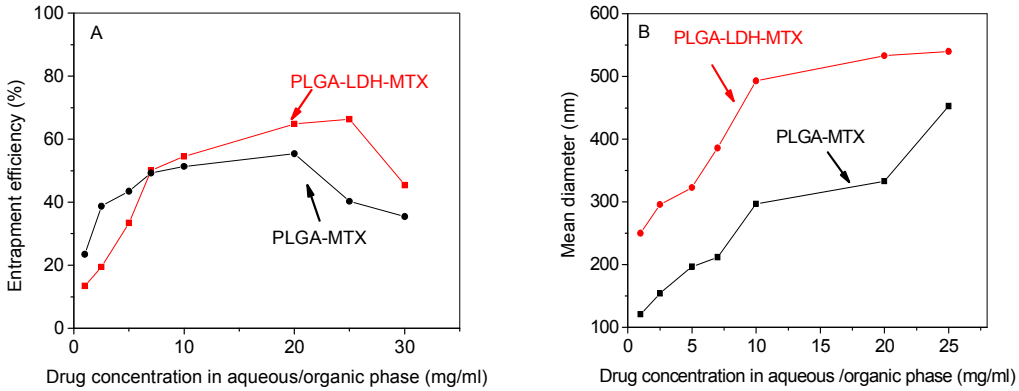

Fig. 6 Effect of drug concentration in organic/aqueous phase on (A) Percentage entrapment efficiency and (B) Particle size of PLGA-MTX and PLGA-LDH-MTX nanoparticles.

It was found that as the concentration of methotrexate increases in the organic phase with polymer, the entrapment efficiency and particle size increase gradually upto certain limit and then decreases. Similar trends were also observed for the case of LDH-MTX in aqueous phase. The drug content in the nanoparticles is affected by the drug–polymer interactions and the drug miscibility in the polymer. It is already reported that higher drug–polymer miscibility leads to higher drug incorporation.[70] In the present case, increasing the initial drug concentration beyond the limit of drug miscibility leads to constant drug content that hinders any excess amount of drug incorporation and hence, the resulting entrapment efficiency decreases.[70,71]

Fig. 6, panel B shows that an increase in loading of the drug increases the mean diameter of the nanoparticles alongwith their polydispersity index. It can be explained that the greater amount of drug results in a highly concentrated dispersed phase, making the mutual dispersion of the organic and the aqueous phases difficult, thereby forming larger particles.[59,72,73]

After optimization of all the process parameters the optimized PLGA-MTX nanoparticles were evaluated for the determination of the residual surfactant, poly (vinyl alcohol) used in the single-emulsion solvent evaporation method. In this, a fraction of the partially hydrolyzed (87-90%) PVA used as surfactant to stabilize the emulsion forms a strong network on the PLGA surface using its hydrophobic vinyl acetate copolymer part as an anchor at the oil-water interface, for binding to the PLGA surface as above, and this could not be removed.[74] This part was estimated to be 20 µg/g of the optimized formulation of PLGA-MTX nanoparticles, following the method as demonstrated in the experimental section.

The experimental yield of the optimized batch of (Table. 3) PLGA-MTX was 66.9%, for PLGA-LDH-MTX was ~71.43%. See eqn S4 and S5 in ESI.

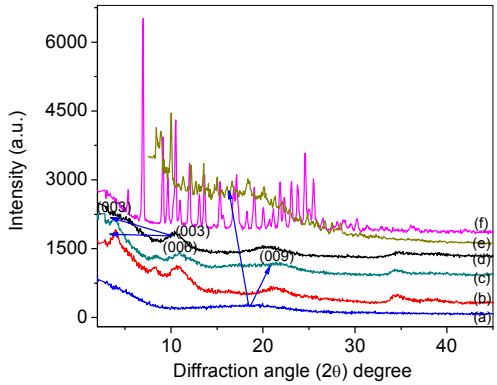

Fig. 7 Powder X-ray diffraction patterns of (a) PLGA (b) LDH–MTX (c) PLGA-LDH-MTX (d) LDH (e) PLGA-MTX (f) MTX.

The powder X-ray diffraction (XRD) patterns of PLGA polymer, pristine-LDH, LDH-MTX and the optimized batches of the PLGA- LDH-MTX and PLGA-MTX nanoparticles are shown in Fig. 7. The pattern is characteristic of the hydrotalcite-like phase comprising hexagonal lattice with rhombohedral space group.[38,40] The d spacing corresponding to the (003) plane of pristine LDH at 8.25 Å (Fig. 7 d) shifted considerably on intercalation of the methotrexate drug to 21.35 Å (Fig. 7 b and c), approximately, marked by a pair of arrows in LDH-MTX and PLGA-LDH-MTX, confirming the encapsulation of LDH-MTX as prepared within the PLGA coating. Considering the thickness of the brucite layers to be 4.8 Å, the gallery height of the LDH-MTX nanohybrid material is found to be (21.35-4.8) Å = 16.55 Å (Scheme-1, X′ Å). The longitudinal molecular length of MTX

is 21.2 Å; hence, the drug molecule is tilted at an angular configuration of 51.5° within the layered framework of the brucite and is held in place by a charge based interaction between the anionic counterpart of the MTX drug and the cationic brucite layers.[38, 39] The pristine LDHs exhibited a series of well developed *(0 0 l)* reflections (Fig. 7 d, JCPDS file No. 350964), which were also clearly seen with both the PLGA coated and the uncoated LDH-MTX (Fig. 7b and c). Almost similar PXRD patterns could be obtained in the cases LDH-MTX and its PLGA coated counterpart (Fig. 7 b and c), except for the hump like peak at around 20° of the diffraction angle, marked by arrow (Fig. 7 c), due to the presence of PLGA polymer (Fig. 7 a).[75] The high intensity peaks at 2θ=13.5, 14.3, 19.4, 27.8 and 30˚ in Fig. 7 (f) confirm the crystalline nature of the pure drug, MTX[76, 77] whereas, in Fig. 7 (e), presence of a small hump corresponding to the PLGA[78] matrix is supported in turn by the above peaks of both low and medium intensities of MTX drug, for PLGA-MTX structure, suggesting molecular dispersion of the MTX drug in the PLGA polymer matrix.

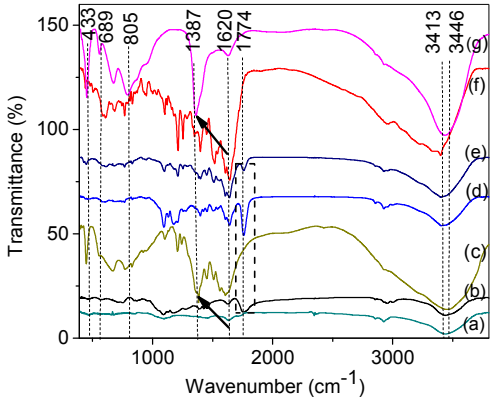

Fig. 8 FTIR spectra of (a) PVA(b) PLGA (c) LDH-MTX (d) PLGA-MTX (e) PLGA-LDH-MTX (f) MTX (g) LDH

Fig. 8 exhibits the major vibration bands corresponding to the compositions as mentioned. Fig. 8 (b) shows vibration bands of PLGA, due to stretching of alkyl group (2850-3000 cm^{-1}), carbonyl C=O stretching (1700-1800 cm^{-1}), C–O stretching (1050-1250 cm^{-1}) due to presence of ester group and –OH stretching (3200-3500 cm^{-1}).[79, 80] The broad hump at 3435 cm^{-1} in Fig. 8 (g) is due to the stretching vibration of both structural hydroxyl and interlayer water molecules of the brucite layers of pristine LDH.[37-39,41] The bands of medium intensity in the lower frequency range from 433 to 689 cm^{-1}, were due to M–O vibration and M–OH bending of the brucite-like layers, while the presence of a band of high intensity at 1387 cm^{-1} signifies the presence of NO_3^- anions in the interlayer space of pristine LDH (arrow marked). Interestingly, the intensity of this band was reduced considerably in LDH-MTX (Fig. 8 c), shown by arrow, suggesting intercalation of the drug molecule leading to partial removal of the NO_3^- anion.[37,38,41] This is in corroboration with the presence of symmetric and asymmetric stretching vibration of the carboxylate group of MTX at 1370 and 1545 cm^{-1} respectively, due to -COO (ν_{COO^-}), and at 1409 and 1620 cm^{-1} due to C=C stretching of MTX,[40,81,82] confirming MTX intercalation in LDH-MTX, as above. Other vibration bands of low and medium intensity are in line with our previous works. The vibration band of medium intensity at 1774 cm^{-1} is attributed to C=O stretching of the PLGA (Fig.8d) hydrocarbon chain, remains almost unaltered in PLGA coated MTX/LDH-MTX nanoparticle, confirming no chemical interaction or bond formation between the PLGA coating and the encapsulated LDH-MTX/MTX (Fig. 8 d,e), marked by a dotted rectangle. In addition to this, the vibration bands of low intensities corresponding to C=C stretching of MTX at around 1620 cm^{-1} is a good proof of the successful entrapment of MTX, both in PLGA-MTX and PLGA-LDH-MTX nanoparticles (Fig. 8 d and e). No significant peak corresponding to the presence of PVA (Fig. 8 a) adsorbed on the PLGA-MTX nanoparticles could be marked in the characteristic pattern of PLGA-MTX (Fig. 8 d).[37] This could be attributed to the negligible amount of the residual PVA present in the optimized formulation of PLGA-MTX nanoparticles. Fig. 8(f) exhibits the major peaks of MTX at 3413 (-NH stretch), 1654 cm^{-1} (-COOH), 1639 cm^{-1}(-CONH), 805 cm^{-1} (aromatic stretch out- of- plane bend), confirming the purity of the drug.[82]

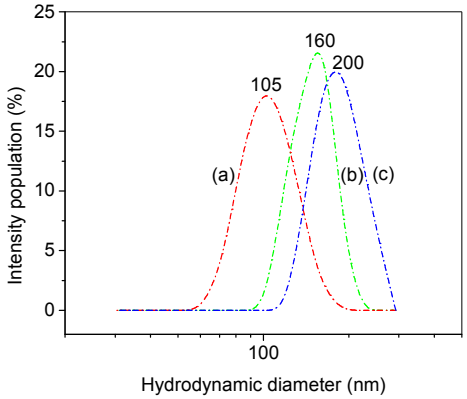

Fig. 9 Particle size distribution (intensity) of (a) PLGA (b) PLGA-MTX (c) PLGA-LDH-MTX of the optimized batch of nanoparticles.

The optimized nanoparticles as above were evaluated for particle size and zeta potential and the results of the same are shown in Table 1 below and the size distribution is depicted in Fig.9, it is evident that with increase in polymer concentration in MTX/LDH-MTX coating, corresponding particle size was found to be increasing up to a certain concentration of polymer with increased polydispersity index (PDI). Finally, in the optimized batch, comprising 2:1 (w/w) PLGA : MTX /PLGA:LDH-MTX ratio, the particle size was found to be 120-180 nm for PLGA-MTX and 180-250 nm for PLGA-LDH-MTX (Fig. 9 b, c) with PDI of 0·163 and 0.217, respectively. The zeta potential values for optimized batch of PLGA-MTX and PLGA-LDH-MTX were found to be in the range of −38·34 and −33·62 mV respectively, indicating excellent stability of the nanoparticles in aqueous suspension.[37, 41] The negative zeta potential values are due to presence of end terminal carboxylic acid group in PLGA and from carbonyl group of PLGA block.[83] The advantage of this negatively charged particle size over positively charged one, lower induction of inflammation than positively charged particle and lower induction of T-cell proliferation and cytokines production and secretion compared to the cationic nanoparticle, hence, causes less damage to the erythrocyte membrane.[84,85] Size distribution pattern of particles plays an important role in determining the drug release behavior, their feasibility for intravenous administration as well as their fate *in vivo*. Due to smaller particles (<200 nm), they tend to accumulate in the tumor sites due to the facilitated extravasations, which can prevent spleen filtering.[86,87] Further a lower PDI indicates enhanced homogeneity of the nanosuspension which was observed with both PLGA-MTX and PLGA-LDH-MTX systems as above.[37]

Table 1 Physiochemical properties of the optimized batches of PLGA-MTX and PLGA-LDH-MTX

Formulation	Drug : Polymer ratio (w/w)	Particle size (nm)	Zeta potential	% Yield	% DEE
PLGA-MTX	1:2	165± 1.37	-38.34	66.9±0.34	35.20± 4.62
PLGA-LDH-MTX	1:2	205± 2.79	-33.62	71.43±2.84	65.12± 3.26

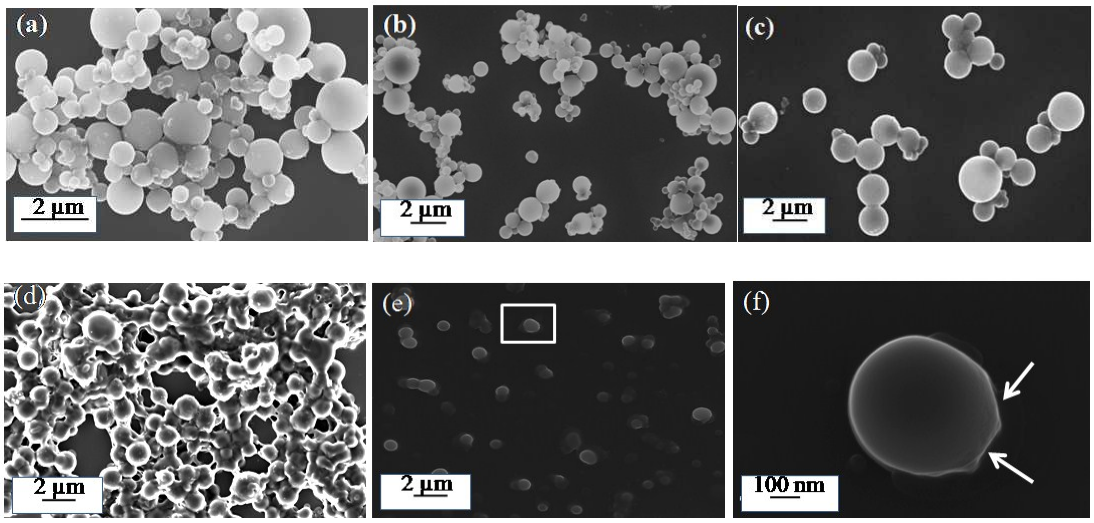

Fig. 10 FESEM micrographs of PLGA-MTX having PVA emulsifier/stabilizer concentration (a) 0.25% (w/v) (b) 1% (w/v) and (c) 2% (w/v), showing the present one as the optimized batch. In case of PLGA-LDH-MTX, the agglomerated nanoparticles having tween 80 concentration (d) 0.15% (w/v) (e) 2% (w/v), showing the optimized batch having discrete, agglomeration free particles having globular morphology (f) a higher magnification image of a marked area (rectangle), exhibits the presence of an almost elliptical PLGA-LDH-MTX nanoparticle, that reveal the presence of a hexagonal plate of LDH-MTX (arrow marked) in the PLGA encapsulated structure.

FESEM images in Fig. 10 depict a wide variation in the size and shape of the particles formed under different process parameters, e.g., homogenization speed, stabilizer concentration etc. Without the LDH nanoparticles, the optimized batch of PLGA coated MTX system exhibit globular morphology forming cluster of the particles with a wide variation of size, e.g., 250 nm to 1.5 µm, shown in Fig. 10 (a). In single emulsion technique for the preparation of PLGA-MTX, the use of low concentration (0.25% w/v) of the water soluble emulsifier, poly (vinyl alcohol), is unable to reduce the interfacial tension between the lipophilic and hydrophilic phases of the microemulsion,[88] leading to aggregation and cluster formation of the resulting nanoparticles, as obtained. A four times increase in the PVA concentration leads to better dispersion of the particles, as shown in Fig. 10(b), whereas, with an eight times increase as above, Fig. 10 (c) exhibit PLGA-MTX almost uniform particle distribution, without much aggregation. However, the presence of the polar hydrogen bond in the aqueous dispersion phase of the emulsion leads to flocculation of the particles to some extent, as is evident from Fig. 10 (c).
In case of PLGA-LDH-MTX, Fig. 10 (d) reveals much aggregated particles, on account of a low concentration (0.15% , w/v) of the hydrophilic emulsifier, tween 80 (HLB value: 15) in the aqueous phase of the secondary emulsion. An increase in concentration to an extent of more than ten times for the optimized batch, Fig. 10 (e) exhibits the presence of aggregation free, discrete and monodisperse PLGA-LDH-MTX particles in the external aqueous phase. Interestingly, on dispersion of the internal/dispersed phase (W_1/O) in the continuous medium (W_2), the entropy of the system is enhanced quite a few times. This is taken care of by the substituted side chain of tween 80, by entrapping the particles leading to dispersion of the same without any aggregation having the minimum surface area, leading to almost round shaped morphology, in the size range 180-250 nm, coated with PLGA. This corresponds to the optimized batch of the synthesis, w.r.t to all the experimental parameters, as abovementioned, that matches with our observation with regard to particle size analysis using DLS (Fig. 9). Fig. 10 (f) confirms the presence of LDH-MTX nanocrystals within the PLGA encapsulated structure, exhibited by the edge of a regular plate like shape, as show by the arrow mark.[37]

Fig. 11 (a) exhibit encapsulation of MTX drug in PLGA polymer of the optimized batch. In presence of PVA as the non ionic emulsion stabilizer/emulsifier, the hydroxyl groups, -OH, can be specifically adsorbed on the emulsion droplet, thus results in formation of a charge, that paves the way for an electrical double layer formation and thereby leading to mutual repulsion between the emulsified particles. However, in the aqueous external phase, the hydrogen bonded network plays a role to flocculate the emulsified PLGA-MTX particles so to obtain clusters as shown in Fig. 11 (a). SAD pattern of the particles as above said, shows diffuse rings, characteristic of the presence of the amorphous PLGA polymer (Fig. 11b). In another image, a magnified view exhibits a discrete particle having perfectly spherical morphology, with a smooth surface, comprising the drug within the polymer encapsulation (arrow marked) as it is evident from Fig. 11 (c).

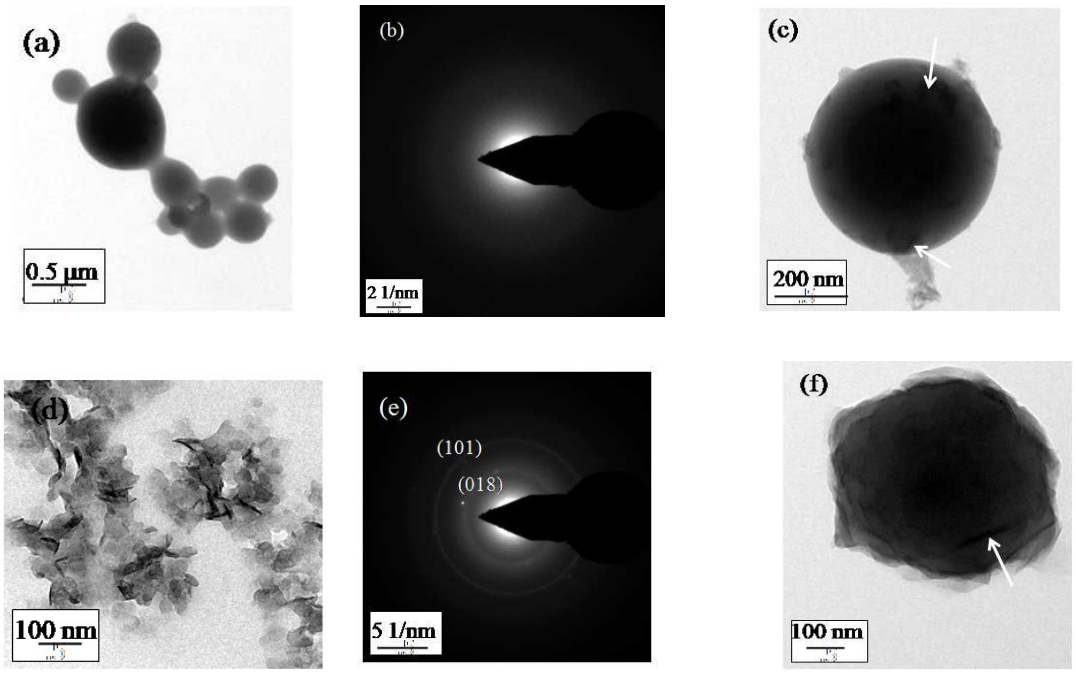

Fig. 11 TEM images of the optimized batch of (a) PLGA-MTX (b) SAD pattern (c) discrete particle having globular morphology, comprising MTX drug in the PLGA encapsulation (arrow marked), at higher magnification (d) Optimized batch of PLGA-LDH-MTX (e) SAD pattern showing the presence of characteristic atomic planes (f) a discrete PLGA coated particle showing the presence of LDH crystals (arrow marked), loaded with MTX, at higher magnification.

In case of LDH-MTX counterpart, Fig. 11(d) exhibits the optimized batch of the nanoparticles precipitated by the double emulsion solvent evaporation method as detailed above. An optimum concentration of the nonionic surfactant, tween 80 (PEG-20 sorbitan monoleate), with high HLB value (15), facilitates agglomeration free dispersion of the oil based dispersed phase, after solvent evaporation, leading to encapsulation of the LDH-MTX nanoparticles in the PLGA coating. Fig. 11(e) exhibit the SAD pattern of the PLGA-LDH-MTX nanoparticles, showing a pair of the (*00l*) reflections characteristic of the LDH-MTX structure, corroborating our findings of the XRD analysis, shown in Fig. 7 (b).[40] A discrete PLGA-LDH-MTX particle shown in Fig. 11 (f) exhibits the planar structure of the LDH-MTX nanohybrid embedded in the polymer matrix (arrow marked).See FigS2 for EDX data of PLGA-LDH-MTX.

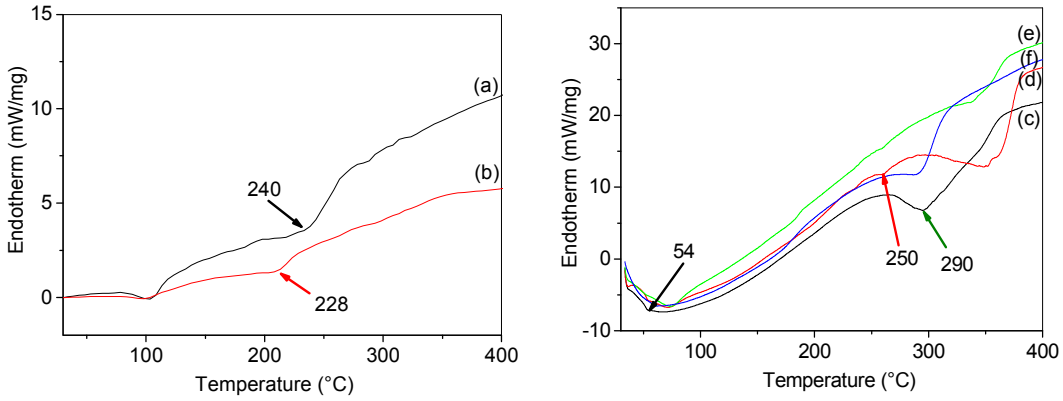

Fig. 12 DSC of (a) MTX (b) LDH-MTX (c) PLGA (d) PLGA-MTX physical mixture (e) PLGA-MTX and (f) PLGA-LDH-MTX nanoparticles.

DSC thermogram of MTX in Fig 12 (a) shows a broad endothermic melting peak at around 240°C [89], but in case of LDH-MTX nanoparticles, the drug melting peak was shifted to lower temperature of 228°C, on account of the melting of the crystalline drug and formation of dispersion at molecular level within the ceramic matrix, confirming the entrapment of the same in the LDH interlayer space. In case of PLGA, an endothermic peak at ~ 54° C corresponds to its glass transition temperature in the range of 40-60°C.[73] A second hump of PLGA at around 290 °C is due to the evaporation of the monomer D, L-lactide.[42,90,91] In case of the physical mixture of PLGA and MTX (1:1 ratio) a small endothermic hump was observed at 250° C corresponding to the melting endotherm of the pure drug. In case of the optimized PLGA-MTX and PLGA-LDH-MTX nanoparticles, absence of the melting peak of methotrexate confirm that drug crystals completely dissolve inside the polymeric matrix or ceramic-polymeric conjugate matrix during the scanning of temperatures up to the melting value or because the drug remained dispersed at molecular level inside the nanoparticles.

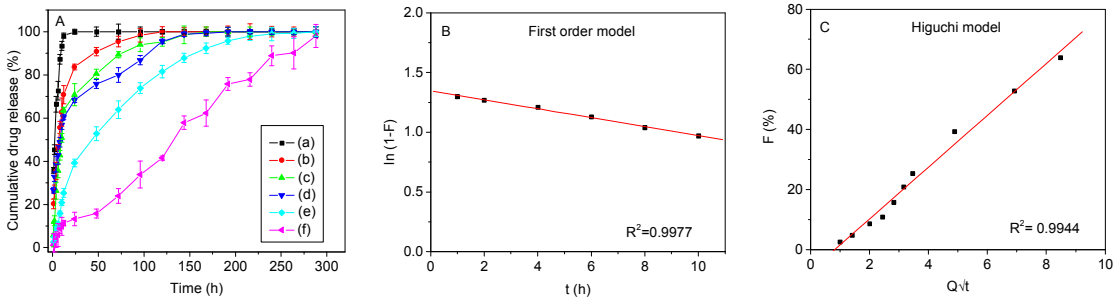

Fig.13 (A) Cumulative release profile of (a) unoptimized PLGA-MTX (L) (b) PLGA-MTX optimized (c) PLGA-MTX (H) (d) PLGA-LDH-MTX (L) (e) PLGA-LDH-MTX optimized (f) PLGA-LDH-MTX (H) nanoparticles (B) First order plot of PLGA-MTX (C) Higuchi plot of PLGA-LDH-MTX.

The drug release from a nanoparticulate matrix system, in which the drug is uniformly embedded, generally occurs by diffusion or erosion of the matrix. Several parameters can affect the drug release rate from matrix systems, in addition to the particle size, molecular weight and ratio of the constituent monomers, e.g., lactide to glycolide ratio of the polymer used as matrix also, influences the drug release kinetics to a large extent.[92, 93] In the present study, the *in vitro* drug release study was carried out in phosphate buffer saline (PBS) of pH 7.4 for some of the selected unoptimized PLGA-LDH-MTX and PLGA-MTX formulations, compared to the corresponding optimized ones, to understand and compare the possible differences in the *in vitro* drug release profile. Herewith, PLGA-MTX (L) (Fig. 13, panel A, subpanel a) corresponds to lower particle mean diameter (< 120 nm) with low drug entrapment efficiency, exhibiting faster release of the drug from the matrix system within 12h period due to higher surface area (on account of lower particle diameter) and low entrapment efficiency.[57] On the other hand, in case of PLGA-MTX (H) (Fig. 13, panel A, subpanel c) corresponds to high entrapment efficiency with higher particle size (~ 2 µm) (Table 3) , leading to slower release of the drug for a much longer period of 144 h, which is much higher than our desired value (120-180 nm as above). In case of PLGA-LDH-MTX unoptimized formulations [PLGA-LDH-MTX (L) and PLGA-LDH-MTX (H)]exhibited at subpanels (d) and (f) of Fig. 13 (A), almost similar pattern as above could be obtained, as discussed. All the relevant physicochemical properties of the unoptimized PLGA-MTX (L&H) and PLGA-LDH-MTX (L&H) are enlisted in Table 3.

The cumulative release profile of the optimized PLGA-MTX nanoparticles exhibited in Fig. 13, panel A, subpanel b, shows an initial burst release pattern. In case of PLGA-MTX, 90.67% of the encapsulated methotrexate was released during the first two days, followed by slower release rate (10%) upto a period of 5 days, exhibiting a biphasic release pattern. In the first phase, the low molecular weight PLGA polymer used in the present case undergoes fast hydrolysis in the release medium, leading to loosening of the polymer chains and thereby fast diffusion of the entrapped methotrexate drug through the empty pores formed, within a short period of time. For the low molecular weight polymer, PLGA as in the present case, the lower chain length lowers its lipophilicity, resulting in lower solubility of the methotrexate drug in the polymer, initiating the burst release of a substantial amount of drug (90.67%) during the first two days only. In phase 2, the rate of diffusion as above becomes much slower being close to equilibrium condition. [94]

In case of optimized PLGA-LDH-MTX, a similar biphasic release pattern could be observed, as shown in Fig. 13, panel A, subpanel e. In this, during the first 5 days, 81.50% of methotrexate was released at a constant and fast rate. Following this, a slower release rate could be observed and nearly 18.50% of the drug was released in next 7 days. In phase 1, the surface adsorbed drug is released fast into the aqueous phase, contributing to the burst release, although it is slower compared to PLGA-MTX on account of loosening of the PLGA chain followed by slow diffusion of the MTX drug, intercalated within the interlayer space of LDH matrix by anion exchange process only . In phase 2, complete rupture of the PLGA chain takes place, leading to exposure of the remaining LDH-MTX in the structure, in contact with the release medium, followed by diffusion of the drug slowly into the same by anion exchange process.[37] Hence, as is clearly evident, the drug release in the case of PLGA-LDH-MTX is extended for a longer period of time compared to PLGA-MTX, on account of the presence of the entrapped LDH-MTX nanohybrid, which facilitates release of the MTX drug from its interlayer space only by anion exchange mechanism, in both the phases of release.[37]

To know the exact release mechanism data obtained from *in vitro* release studies were fitted into various kinetic equations[95-97] (Table 2) to find out the mechanism of methotrexate release from both PLGA-LDH-MTX and PLGA-MTX. On fitting all the four kinetic models in the release kinetic data of methotrexate, it was found that the Higuchi model is the most satisfactory for describing the mechanism of the release of metholtrexate from the PLGA-LDH-MTX at pH 7.4, with correlation coefficient values 0.9944 (Fig.13 panel C). This indicated that the release of MTX from PLGA-LDH-MTX followed diffusion controlled release.[97] Further, the drug release data was fitted to Korsmeyer-Peppas (K-P) model to determine the value of diffusion exponent (n). The value of n for a spherical system, <0.43 indicates Fickian release, $0.43<n<0.85$ indicates non-Fickian release; $n> 0.85$ indicates case II release.[96] The n-value obtained for PLGA–LDH-MTX after the K-P plot was in the range of 0.43–0.85 indicating that release followed anomalous non Fickian transport, it could be suggested that the release is related to combination of both diffusion and dissolution process.[96,98] For PLGA-MTX, the correlation coefficient of 0.9977 (Fig. 13 panel B) indicates first order model of release kinetics of methotrexate, i.e., the cumulative release of the drug is directly proportional to the concentration of the same in the PLGA polymer matrix.[95] From the K-P model, it was found that PLGA-MTX formulation ($n=0.504$) showed an anomalous transport kinetics i.e., a combined mechanism of pure diffusion and dissolution. The calibration curve of MTX in PBS and some other fitting plots of MTX release from the optimized batches of PLGA-MTX and PLGA-LDH-MTX nanoparticles are shown in Fig S3 and S4 of ESI.

Table 2 Correlation coefficients (R^2) of different model of release kinetics of optimized batches of PLGA-MTX and PLGA-LDH-MTX

Optimized nanoparticles	Zero order	First order	Higuchi	Korsmeyer Peppas	*n* values
PLGA-MTX	0.9968	0.9977	0.9950	0.9907	0.504
PLGA-LDH-MTX	0.9629	0.9897	0.9944	0.9914	0.74

Table 3 Physiochemical properties of the un optimized PLGA-MTX (L&H), PLGA-LDH-MTX (L&H) nanoparticles where the drug:polymer ratio and other process parameters are constant and the homogenization speed only was varied (for unoptimized nanoparticles)

Formulation	Drug : Polymer ratio (w/w)	Homogenization speed (rpm)	Particle size (nm)	Zeta potential	% Yield	% EE
PLGA-MTX- L	1:2	15,000	112 ± 1.79	-32.04	45.40 ± 1.74	15.84 ± 2.16
PLGA-MTX-H	1:2	5,000	1865 ± 1.90	-34.14	59.33 ± 3.39	62.28 ± 1.33
PLGA-LDH-MTX-L	1:2	15,000	110 ± 2.22	-33.76	51.33 ± 6.14	4.39 ± 4.36
PLGA-LDH-MTX-H	1:2	5,000	1980 ± 3.43	-34.33	63.88 ± 1.09	89.96 ± 4.56

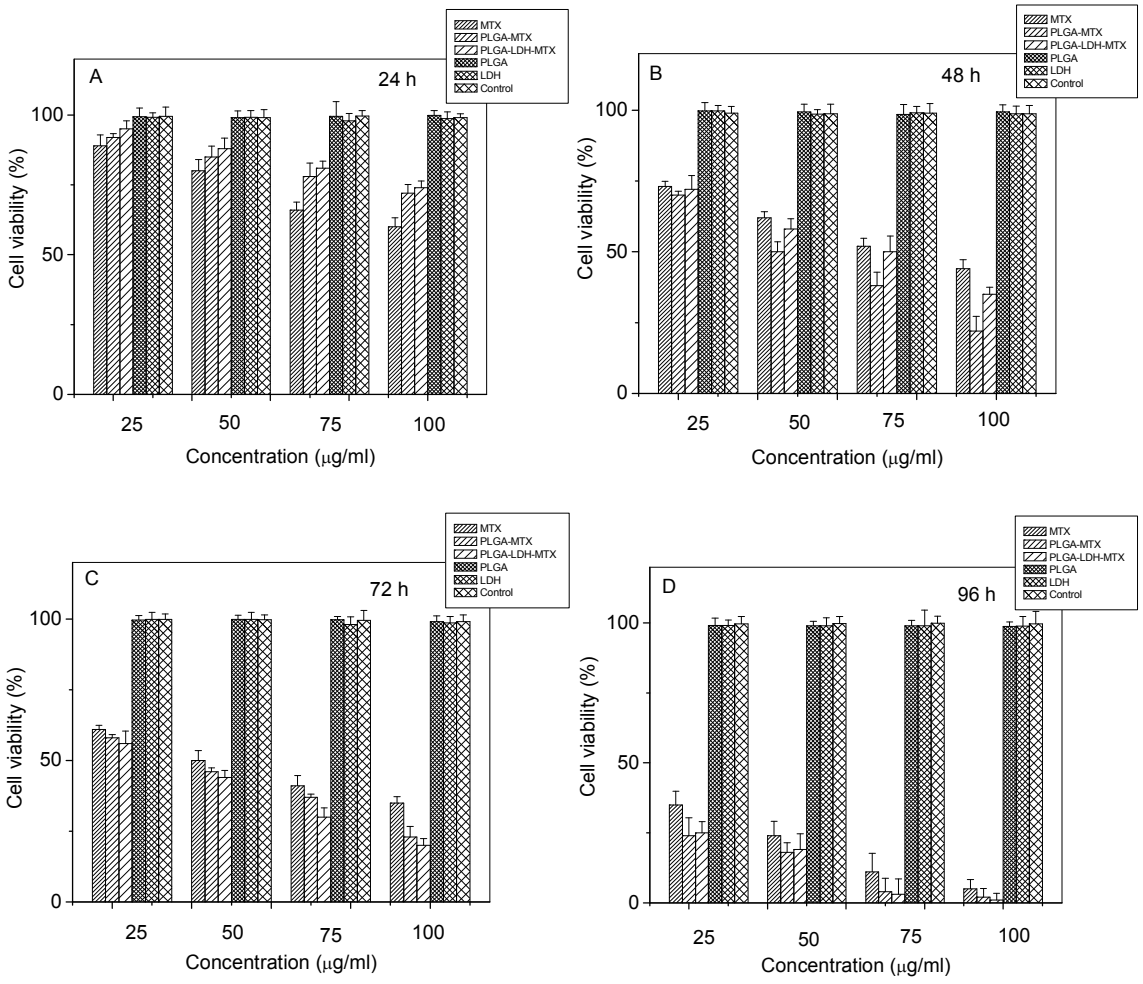

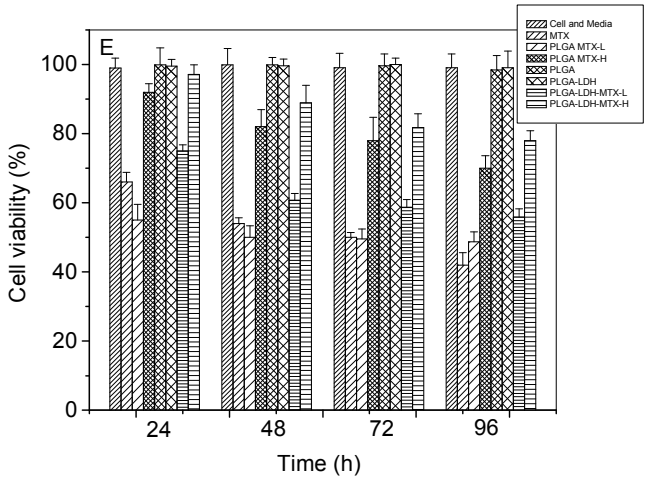

Fig.14 *In vitro* cell viability of the optimized batches of PLGA-MTX, PLGA-LDH-MTX nanoparticles w.r.t PLGA, LDH and MTX at four different time points of (A) 24 h (B) 48 h (C) 72 h and (D) 96 h, showing the highest efficacy of the PLGA-LDH-MTX nanoparticles by the time period of 96h. Panel E shows the *in vitro* cell viability at a fixed dose (75 μg/ml), taking into account the unoptimized formulations, e.g., PLGA-MTX (L), PLGA-MTX (H), PLGA-LDH-MTX (L) and PLGA-LDH-MTX (H) respectively.

The *in vitro* cell viability assays are carefully considered before a new formulation can be tried in animal or human subjects. Such methods are primarily employed to identify potentially hazardous chemical substances and to confirm the lack of toxicity at the early stages of development of potentially useful new therapeutic.[37,99] Based on this concept, in the present study, we have measured how effective the PLGA encapsulated systems, PLGA-MTX and PLGA-LDH-MTX nanoparticles are to inhibit the growth of the bone cancer cells, in a time and dose dependent manner. Hence, four different trial concentrations of the drug MTX, PLGA, LDH, PLGA-MTX, PLGA-LDH-MTX were studied in the multiple of 25, e.g., 25, 50, 75 and 100 μg/ml, at four different time points of 24, 48, 72 and 96 h on human osteosarcoma cell line, MG-63 (Fig. 14). The concentrations mentioned herewith were chosen randomly to undertake the trial experiment as above for estimation of efficacy of the newly developed nanoparticles, PLGA-MTX and PLGA-LDH-MTX. Interestingly, the results revealed more than 97% cell viability for the cases using PLGA and LDH, confirming their nontoxicity[100,101] for the encapsulation of MTX or LDH-MTX, irrespective of time and dose. However, the optimized nanoparticles, PLGA-MTX and PLGA-LDH-MTX exhibited cytotoxicity in a time and dose dependent manner, along with MTX. At 24h, almost no effect of the same could be observed on the human osteosarcoma cells, whereas, on completion of two days (48 h), a marked reduction on cell viability (≈50%) was observed when MG-63 cells were incubated with 100 μg/ml of pure MTX at 37 ºC, whereas for PLGA-MTX it showed ≈50% cell inhibition at half the concentration as above (50 μg/ml) and around 60% cell inhibition at 75 μg/ml, around 70% inhibition at 100 μg/ml respectively (Figure 14, panel B). On the contrary, at the same time period (48 h), PLGA-LDH-MTX nanoparticles exhibit 50 % cell inhibition only at the higher concentration range of 75 and 100 μg/ml. As evident, PLGA-MTX nanoparticles show better result compared to bare MTX and PLGA-LDH-MTX at 50, 75 and 100 μg/ml concentrations on account of their smaller particle size (120-180 nm) that leads to easy cellular uptake through the anionic cell membrane, by endocytosis mechanism. This corroborates with our observation at 72h (Fig. 14, panel C). Longest incubation time of 96 h was also considered in our work, based on the slow and controlled release of MTX from the polymer coated PLGA-LDH-MTX system that indicates the possibility of better efficacy of the same in an extended time period (Fig. 14, panel D). It was clearly observed that both the polymer coated formulations, PLGA-MTX and PLGA-LDH-MTX inhibit the cancer cell growth at a much higher scale compared to bare MTX, at concentrations of 50, 75 and 100 μg/ml. Interestingly, incubation time is a critical factor here: at 24h, no significant effect could be noticed for the above polymer coated optimized formulations at concentration range of 50, 75 and 100 μg/ml , while, after a period of 96 h incubation, a marked reduction in cell viability could be achieved, up to the extent of 90-95%.Hence, the present study not only shows the time dependent efficacy of the optimized polymer coated nanoparticles compared to bare MTX drug on MG-63 cells, but also indicates that the lower doses (e.g., 75 μg/ml) of the optimized batches of PLGA-MTX and PLGA-LDH-MTX nanoparticles are better than the higher dosage (e.g., 100 μg/ml) of pure MTX in a time period of 96h.[102]
For unoptimized formulations corresponding to the optimized PLGA-MTX and PLGA-LDH-MTX, in the present case, we have considered PLGA-MTX (L) and (H) as well as PLGA-LDH-MTX (L) and (H) respectively, for the *in vitro* cell viability study using human osteosarcoma (MG-63) cell line. Herewith, we have taken into account a fixed concentration of MTX drug at 75 μg/ml, at four different time points of 24, 48, 72 and 96 h. The concentration of the drug as above was fixed based on our earlier data as exhibited in panel A to D of Fig. 14, which confirms the highest efficacy of both the optimized formulations of PLGA-MTX and PLGA-LDH-MTX nanoparticles in a period of 96 h. In case of PLGA-MTX (L) and PLGA-LDH-MTX (L), the smaller particle mean diameter (< 120 nm) aids in faster endocytosis of the nanoparticles alongwith faster release of the drug within the cancer cell, leading to a consolidated effect (cancer cell growth inhibition of around 50-55%) of the same during the time period of 24 to 96 h.For PLGA-MTX (H) and PLGA-LDH-MTX (H), higher particle mean diameter (size range: 800 nm to

2 μm) hinders the endocytosis mechanism and at the same time, slow release of the drug, outside the cell, in the DMEM medium leads to slow diffusion of the drug into the cell and hence the delay in the growth inhibition process (20-30% in a period of 24 to 96 h).
For the concentrations 25 and 50 μg/ml in the lower range and 100 μg/ml in the higher range, the *in vitro* cell viability assay was carried out using the unoptimised set of formulations [PLGA-MTX (L) and (H) and PLGA-LDH-MTX (L) and (H)] and we obtained statistically insignificant results which could not be presented here.

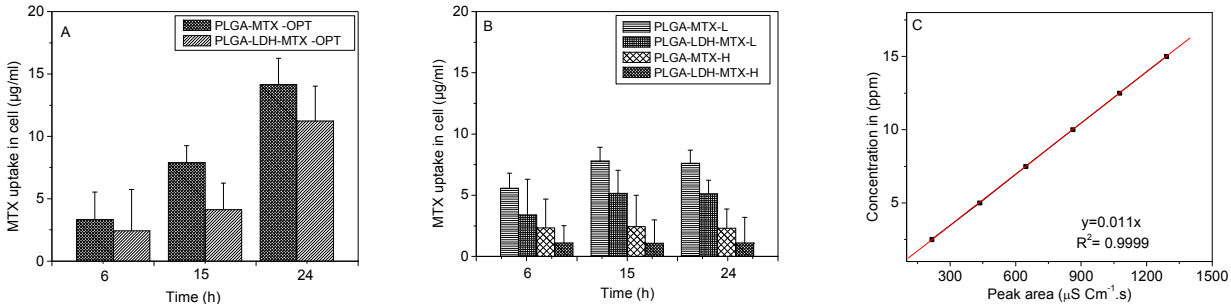

Fig. 15 *In vitro* MTX uptake study of (A) optimized PLGA-MTX and PLGA-LDH-MTX nanoparticles (B) unoptimized PLGA-MTX (L &H) and PLGA-LDH-MTX (L&H) nanoparticles using MG-63 cell line at three different time points. (C) Calibration curve of MTX drug

The cellular uptake of MTX drug from the optimized PLGA-MTX and PLGA-LDH-MTX nanoparticles in MG-63 cell line at three different time points of 6, 15 and 24 h respectively is shown in Fig. 15, panel A. The study exhibits that the drug uptake was significantly increased with respect to time in both the cases as above. However, in case of PLGA-MTX, on account of its smaller particle size (120-180 nm), faster insertion in the cell takes place by endocytosis mechanism compared to PLGA-LDH-MTX. This leads to higher cellular uptake in terms of quantity of MTX (3.34 μg/ml at 6 h, 7.91 μg/ml at 15 h and 14.15μg/ml at 24 h) in the former case whereas, in the later case, not only the larger particle size (180-250 nm) hinders the insertion of the same in the cell by endocytosis mechanism, but, at the same time, slower release of the encapsulated drug within the cell takes place on account of the presence of a nanoceramic matrix that in turn is coated with PLGA polymer (2.43 μg/ml at 6 h, 4.13 μg/ml at 15 h and 11.24 μg/ml at 24 h).
In case of the unoptimised set of formulations [PLGA-MTX (L) and (H) and PLGA-LDH-MTX (L) and (H)] (Fig. 15, panel B), we had compared PLGA-MTX (L) with PLGA-LDH-MTX (L) and obtained that the MTX uptake in the cell from the above nanoparticles is following a slight increasing trend at the initial time points of 6 and 15 h, on account of endocytosis and hence MTX release from a large number of nanoparticles (due to small size, <120 nm) (Table 3) whereas, not much distinct differences could be observed at 24 h, on account of the low entrapment efficiency (Table 3) of the same. In case of the unoptimized PLGA-MTX (H) and PLGA-LDH-MTX (H) nanoparticles, the MTX uptake in the cell was almost below detection level on account of the large particle size (800 nm-2 μm) (Table 3), as above leading to minimum/ almost no insertion of the nanoparticles within the cell.

The pharmacokinetic parameters of the optimized batches of PLGA-MTX and PLGA-LDH-MTX were compared with pure methotrexate drug (API), after intravenous administration. The plasma drug concentration profile and the corresponding pharmacokinetic parameters have been summarized in Fig. 16, panel A, B and C and in Table 4. The values of area under the curve-versus-time curve ($AUC_{0-\infty}$, 1.304 mg/h/ml), and $t_{1/2}$ (4.68 h) of PLGA-MTX nanoparticles were found to be much higher (6 times for AUC and 20 times for $t_{1/2}$) than the pure drug MTX ($AUC_{0-\infty}$, 0.266 mg/h/ml, $t_{1/2}$ 0.24 h), after being encapsulated in PLGA. In case of PLGA-LDH-MTX nanoparticles, $AUC_{0-\infty}$ was found 2.155 mg/h/ml and $t_{1/2}$ was 15.4 h which is almost 10 fold w.r.t the corresponding parameter of the pure drug and almost 75 fold w.r.t the $t_{1/2}$ of the pure drug .It is clearly observed that the PLGA-LDH-MTX nanoparticles exhibited longer retention time. The plasma drug concentration for PLGA-MTX nanoparticles was detectable upto 72 h (Fig. 16, panel B) where as for PLGA-LDH-MTX it was detectable up to 200 h (Figure 15, panel C) which may be due to the slow clearance rate leading to enhancement in elimination half life and correlates well with *in vitro* release data.[103] The results showed nanoparticles had significantly improved the exposure, reduced the clearance, and slightly raised the volume of distribution compared to the pure MTX drug.[104] This may be attributed to the sustained release of MTX from PLGA-MTX and PLGA-LDH-MTX nanoparticles respectively. In case of the PLGA-MTX, such release is diffusion controlled, leading to retention of the drug (marked by arrow, Fig. 16, panel B) in the elimination phase, for PLGA-LDH-MTX, release of the drug via anion exchange mechanism leads to longer retention of the same, compared to PLGA-MTX and MTX (marked by arrows, Fig. 16, panel C). The *in vitro* release profile had good correlation to the release results *in vivo* by measuring plasma drug concentration profile in pharmacokinetics experiment by intravenous injection. The reason for sustained release was considered to be nanoparticles were relatively long circulation with low clearance rate when compared to the pure drug. Nanoparticles showed significant changes in pharmacokinetic profile compared to pure drug. It can be observed that there was a

statistically significant difference ($p < 0{\cdot}05$) in pharmacokinetic parameters when MTX was formulated in the form of nanoparticles at 95% confidence interval (CI).

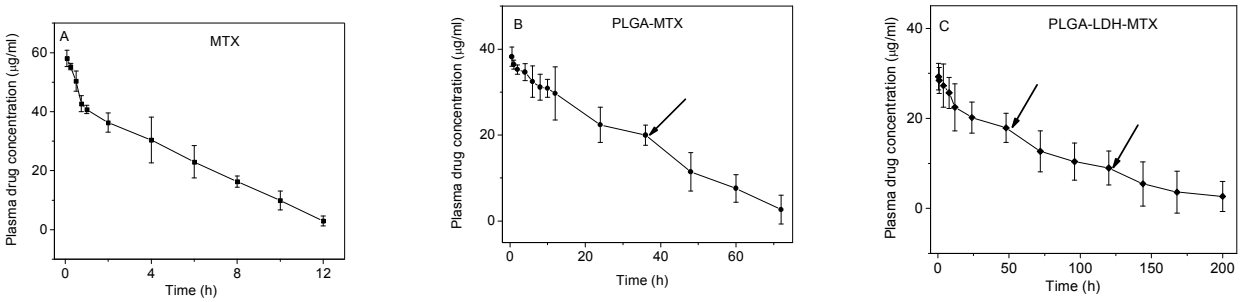

Fig.16 Pharmacokinetic release profile of **(**A) MTX (B) Optimized PLGA-MTX nanoparticles and (C) Optimized PLGA-LDH-MTX nanoparticles.

Table 4 Pharmacokinetic parameters of MTX loaded PLGA-MTX and PLGA-LDH-MTX compared to MTX

PK parameters	Units	(MTX)	PLGA-MTX	PLGA-LDH-MTX
$AUC_{0-\infty}$	µg.h/ml	266.09	1304	2155.5
Elimination half life ($t_{1/2}$)	h	0.24	4.68	15.4
Elimination rate (K_{el})	l/h	2.88	0.148	0.045
Volume of distribution (V_d)	L/Kg	0.406	0.60	0.8
Clearance (Cl)	ml h^{-1} kg^{-1}	0.731	0.0555	0.0225

Conclusion

In the present report, different correlations could be obtained for all the process parameters in discussion for the optimized PLGA-LDH-MTX and PLGA-MTX nanoparticles with regard to their physicochemical properties, for specific use. The XRD data of the above exhibited characteristic peaks to confirm the presence of PLGA coating, methotrexate drug and LDH-MTX nanoparticles. The particle size distribution by DLS, reveals a low PDI indicating a range of 120-180 nm for PLGA-MTX and 180-250 nm for PLGA-LDH-MTX nanoparticles, exhibiting a good stability, marked by their zeta potential of −38•34 and −33•62 mV respectively of PLGA-MTX and PLGA-LDH-MTX nanoparticles, respectively. For both the optimized nanoparticles as above, the effect of surfactant concentration could be correlated with the particle morphology and distribution, by an inverse proportionality, revealed by the electron microscopy studies. The thermal analyses revealed a molecular level dispersion of the MTX drug in the polymer/polymer-ceramic conjugate carrier. The release of MTX from the optimized nanovehicles as above follows Higuchi for PLGA-LDH-MTX and first order kinetics for PLGA-MTX while the maximum efficacy of the above nanoparticles to inhibit the growth of human osteosarcoma cell line was found to be at 96 h, *in vitro*. The superiority of the above optimized formulations were established compared to the unoptimized ones, both in lower and higher range for *in vitro* drug release, cell viability and cellular uptake studies. The *in vivo* pharmacokinetic data exhibited enhanced properties of the above nanoparticles in Newzealand white rabbit model, w.r.t the drug half life, elimination rate constant, clearance rate indicating longer retention of both the optimized formulations compared to bare MTX that confirms the possibility of better efficacy compared to the existing formulation of bare MTX.

Acknowledgements

The authors are grateful to the Director, Central Glass and Ceramic Research Institute, Kolkata, India for providing his permission and facilities to carry on the above work. Thanks are due to all the supporting staffs for various characterization works. This work was supported by the CSIR Twelve Five Year Plan Project ESC 0103 (BIOCERAM).

Notes and references

[a]CSIR-Central Glass and Ceramic Research Laboratory
196, Raja S.C. Mullick Road, Jadavpur, Kolkata-700 032, INDIA

[b]West Bengal University of Animal and Fishery Sciences
37 & 68, Kshudiram Bose Sarani, Belgachia, Kolkata-700037, INDIA

[c]Department of Pharmaceutical Technology, Jadavpur University,
Jadavpur, Kolkata-700 032, INDIA

*Corresponding author: Tel.: +91-33-24733476 (3233); Fax: +91-33-24730957
Email address: jui@cgcri.res.in (Jui Chakraborty)

1 T. A. Damron, W. G. Ward and A. Stewart, *Clinical Orthopaedics and Related Research*, 2007, **459**, 40.
2 L. Mirabello, R. J. Troisi, *Cancer,* 2009, **115,** 1531.
3 A. M. Kurt, K. K. Unni, R. A. McLeod, and D. J. Pritchard, *Cancer*, **65 (6)**, 1418, 1990.
4 K. K. Unni and D. C. Dahlin, *Seminars in Roentgenology*, 1989, **24 (3)**, 143, 1989.
5 R. J. McKenna, C.P. Schwinn, K. Y. Soong, *J Bone Joint Surg (Amer),* 1966, **48**-A, 1.
6 H. D. Dorfman, B. Czerniak, *Bone Tumors*. 1st ed. St. Louis, MO: Mosby; 1998:128
7 N.Marina,M. Gebhardt, L. Teot, and R. Gorlick, *Oncologist*, 2004, **9 (4)**, 422, 2004
8 P. A. Meyers, G. Heller, J. Healey, A. Huvos, J. Lane and R. Marcove, *J Clin Oncolo*, 1992, **10**, 5.
9 G. Bonadonna, S. Monfardini, M. De Lena, F. Fossati- Bellani and G. Beretta,*Cancer Res.*, 1970, **30**, 2527.
10 W. W. Sutow, *Cancer Chemother Rep*, 1975, **6**, 315.
11 W. W. Sutow, E. A. Gehan and P. C. Dyment, *Cancer Chemother Rep*, 1978, **62 (2)**, 265.
12 F. R. Eilber, G. Rosen, *Semin Oncol.,*1989, **16**, 312.
13 M. P. Link, A. M. Goorin, A. W. Miser, *N Engl J Med*.,1986, **314**, 1600.
14 T. Philip, C. Iliescu, M. C. Demaille, H. Pacquement, J. C. Gentet and I. Krakowski, *Ann Oncol.*, 1999, **10 (9)**, 19.
15 G. Bacci, F. Gherlinzoni, P. Picci, J. R. Van Horn, N. Jaffe and A. Guerra, *Eur J Cancer Clin Oncol.*, 1986, **22**, 1337 .
16 T. Anita, Y. Lee and K. Pile, *AustralianPrescriber,* 2003, **26 (2)**, 36.
17 R. J. VanDooren-Greebe, A. L. A Kuijpers, J. Mulder, T. De Boo, *Br. J. Dermatol*, 1994, **130**, 204.
18 T. Pincus, Y. Yazici, T. Sokka, D. Aletaha, J. S. Smolen, *Clin Exp Rheumatol .*,2003, **21 (31)**, 179.
19 F. A. Kincl, L. A. Ciaccio, S. B. Henderson, *Arch Pharm (Weinheim)*, 1984, 317 **(8)**, 657.
20 V. V. Mody, *Internet Journal of Medical Update* 2010, 5 **(2)**, 1.
21 P. K. Dutta, M. N. V. Ravikumar & J. Dutta, *J Macromol Sci Polymer Rev.*, 2002, **42**, 307.
22 H. H. Tønnesen, J. Karlsen, *Drug Dev Ind Pharm.*, 2002, **28 (6)**, 621.
23 H.Q. Mao, I. Kadiyala, K.W. Leong, Z. Zhao, W.B. Dang, *Encyclopedia of controlled drug delivery* ,1999, 45.
24 J. Tamada, R. Langer, *J Biomater Sci Polymer Edn* , 1992, **3 (4)**, 315.
25 T. J. Webster, *Am.Ceram. Soc. Bull.,* 2003, **82**, 23.
26 M. Goldberg, R. Langer and X. Jia, *J Biomater Sci Polymer Edn,* 2007, **18**, 241.
27 U. Kedar, P. Phutane, S. Shidhaye, V. Kadam, *Nanomedicine*, 2010, **6**, 714.
28 M. Biondi, F. Ungaro, F. Qualia, *Adv Drug Deliv Rev* , 2008, **60**, 229.
29 S. J. Choi, J. M. Oh, J. H. Choy, *J. Ceram. Soc. Jpn.,* 2009, **117**, 543.
30 Z. P. Xu, Q. H. Zeng, G. Q. Lu, *Chem Eng Sci,* 2005, **61 (3)**, 1027.

31 Z. P. Xu, M. Niebert, K. Porazik, *J Control Release,* 2008, **130 (1)**, 86.

32 J. H. Choy, S. Y. Kwak, Y. J. Jeong, J. S. Park, *Angew Chemie Int Ed,* 2000, **39 (22)**, 4042.

33 F. Cavani, F. Trifiro, A. Vaccari, *Catal. Today,* 1991, **11 (2)**, 173.

34 P. S. Braterman, Z. P. Xu, F. Yarberry , Layered double hydroxides (LDHs).Handbook of Layered Materials (eds. S.M.Auerbach, K.A. Carrado, P.K. Dutta), CRC Press (New York), 2004, 373.

35 F. Trifiro, A. Vaccari, *Compr Supramolecular Chem.,* 1996, **7**, 251.

36 W. T. Reichle, *Solid State Ionics*, 1986, **22 (1)**, 135.

37 S. Ray, J. Chakraborty, B. Sa and S. Ghosh, *RSC Adv.*, 2015, **5**, 39482.

38 M. Chakraborty, S. Dasgupta, C. Soundrapandian, J. Chakraborty, S. Ghosh, M. K. Mitra and D. Basu, *J. Solid State Chem.,* 2011, **184**, 2439.

39 M. Chakraborty, S. Dasgupta, P. Bose, A. Misra, T. K. Mandal, M. Mitra, J. Chakraborty and D. Basu, *J. Phys. Chem. Solids,* 2011, **72**, 779

40 M. Chakraborty, S. Dasgupta, S. Sengupta, J. Chakraborty, S. Ghosh, J. Ghosh, M. K. Mitra, A. Mishra, T. K. Mandal and D. Basu, *Ceram. Int.,* 2012, **38**, 941.

41 J. Chakraborty, S. Roychowdhury, S. Sengupta and S. Ghosh, *Mater. Sc. Engg. C.,* 2013, **33**, 2168.

42 M. Stang, H. Schumann, H. Schubert, *Eng. Life Sci.*, 2001, **1(4)**, 151.

43 H. Karbstein, H. Schubert, *Chem Eng Process*, 1995, **34**, 205.

44 H. Jeffery, S. S. Davis, *Int. J. Pharm.*, 1991, **77**, 169.

45 K. Musmade, P. B. Deshpande, P.B. Musmade , *Bull. Mater. Sci.*, 2014, **37**, 951

46 R. Herrero-Vanell, L. Ramirez, A. F. Carballido, M. F. Refolo, *Pharm Res*, 2000, **17**, 1323.

47 Y. C. Wangl, *AAPS Pharm Sci Tech*., 2009, **10 (4)**, 1263.

48 S.C. Lee, J.T. Oh, M.H. Jang, S.I. Chung, *J. Controlled Release* , 1999, **59 (2)**, 123.

49 S.K. Sahoo, *J. Controlled Release,* 2002, **82**, 105.

50 R. Freshney, Culture of animal cells: Amanual of basic techniques, 1994, 3rd Edn. New York: Wilyi-Liss, Inc.

51 C. Fonseca, S. S. Simoes and R. Gaspar, *J. Control Release,* 2002 **83** 273.

52 S. K. Shaoo, J. Panyam, S. Prabha, V. Labhasetwar, *J. Control Release*, 2002, **82**, 105.

53 N. Kohler, C. Sun, J. Wang, M. Zhang, *Langmuir* 2005, **21**, 8858.

54 W.A. Ritschel, Hand Book of Basic Pharmacokinetics. 2nd edn. Hamilton, Illinois, 1980,274.

55 A. Moghbel, A. Z. Moghaddam, M. Pedram, *Iran. J. Pharm Res.*, 2003, 149.

56 Y. Javadzadeh, F. Ahadi, S. Davaran, G. Mohammadi, A. Sabzevari, K. Adibkia, *Colloids Surf., B,* 2010, **81**, 498.

57 K. Yoncheva, J. Vandervoort, A. Ludwig, *J. Microencapsul*., 2003,**20**, 449.

58 M. F. Zambaux, F. Bonneaux, R. Gref , P. Maincent, E. Dellacherie, M. J. Alonso, P. Labrude , *J. Control Release*, 1998, **50**, 31.

59 A. Budhian, S. J. Siegel, K. I. Winey, *Int. J. Pharm.,*2007, **336** , 367.

60 R. C Mehta, B. C. Thanoo, P. P. DeLuca, *J. Controlled Release*, 1996, **41**, 249.

61 E J A .M. Schlicher, N. S. Postma, J. Zuidema, H. Talsma, W. E. Hennink, *Int. J. Pharm*., 1997, **153**, 235.

62 R. Bodmeier, J. W. McGinity, *Int. J. Pharm*., 1988**, 43**, 179.

63 H Thakkar, R. K. Sharma, A. K. Mishra, K. Chuttani, R. R. Murthy, *AAPS Pharm SciTech* 2005, **6 (1)**, 12.

64 M. L. T. Zweers, D.W. Grijpma, G. H. M. Engbers, J. Feijen, *J. Biomed. Mater. Res. Part B: Appl. Biomater*., 2003, **66B**, 559.

65 E. Allemann, R. Gurny, E. Doelker, *Int. J. Pharmacol*., 1992, **87**, 247.

66 J. H. Lee, T. G. Park, H. K. Choi, *Int. J. Pharm.,* 2000, **196 (1)**, 75.

67 R. M. Mainardes, R. C. Evangelista, *Int. J. Pharm.*, 2005, **290 (137)**, 144.

68 T. Paul, S. Paul, B.Sa, *Pharmacol. Pharm.*, 2011, **2**, 56.

69 X. Li, X. Deng, M. Yuan, C. Xiong, Z. Huang, Y. Zhang, Y, W Jia, *Int. J. Pharm.,* 1999, **178**, 245.

70 F. Boury, H. Marchais, J. E. Proust, J. P. Benoit, *J. Controlled Release*, 1997, **45**, 75.

71 M. N. V. Ravi Kumar, U. Bakowsky, C. M. Lehr, *Biomaterials*, 2004, **25**, 1771.

72 A. Budhian, S. J. Siegel, K. I. Winey, *J.Microencapsul*., 2005, **22**, 773.

73 J. Panyam, D. Williams, A. Dash, D. Leslie-Pelecky, V. Labhasetwar, *J. Pharm. Sci.,* 2004, **93**,1804.

74 H.Murakami, Y. Kawashima, T. Niwa, T. Hino, H. Takeuchi, M. Kobayashi, *Int. J. Pharm*., 1997, **149**, 43.

75 C. E. Astete, C. M. Sabliov, *J Biomater Sci Polymer Edn* , 2006, **17**, 247.

76 T. W. Hambley, H. K. Chan and I. Gonda, *J. Am. Chem. Soc*., 1986, **108,** 2103.

77 P. A. Sutton, V. Cody and G. D. Smith, *J. Am.Chem. Soc.*, 1986, **108,** 4155.

78 H. Gupta, M. Aqil, R. K. Khar, A. Ali, A. Bhatnagar, G. Mittal, *Nanomed. Nanotechnol. Bio.Med.*, 2010, **6,** 324.

79 C. D. C. Erbetta, R. J. Alves, J. M. Resende, R. F. S. Freitas, R. G. Sousa, *J Biomater Nanobiotechnol*, 2012, 3, 208.

80 J. Kasperczyk, *Polymer*, 1996, **37**, 201.

81 K. Hirenkumar, I. Makadia and J. S. Siegel, *Polymers,* 2011, **3**, 1377.

82 N. Kohler, C. Sun, J. Wang, M. Zhang, *Langmuir,* 2005, **21 (19)**, 8858.

83 I. Bala, V. Bhardwag, S. Hariharan and N. Roy, *J. Drug Target*, 2006, **14**, 27.

84 W. F. Ding, F. Wang, J. F. Zhang, J.F. Y. B. Guo, S. Q. Ju, H. A. Wang, *J Nanotechnology,* 2013, ***24***, 101.

85 T. Nakanishi, J. Kunisawa, A. Hayashi, Y. Tsutsumi, K. Kubo, S. Nakagawa, M. Nakanishi, K. Tanaka, T. Mayumi, *J. Control. Release,* 1999, **61**, 233.

86 A. Potineni, M. D. Lynn, R. Langer, M. M. Amiji , *J. ControlRelease*, 2003, **86** 223.

87 K. Ranjith, *Bull. Mater. Sci*., 2011, **35 (3)**, 319.

88 Y. Y. Yang, T. S. Chung, N. P. Ng, *Biomaterials*, 2001, ***22***, 231.

89 A. R. Chamberlin, A. P. K. Cheung and P. Lim, Methotrexate, in Florey K, (ed), *Analytical profile of drug substances.* 5th Vol. The Academic Press Inc., London, New York, Sanfrancisco. 1976, 283.

90 D. Klose, F. Siepmann, K. Elkharraz and J. Siepmann, *Int. J. Pharm.,* **2008**, 354, 95.

91 H. Kranz, N. Ubrich, P. Maincent and R. Bodmeier, *Int. J. Pharm.,* 2000, **89**, 1558.

92 M. Ramchandani, D. Robinson, *J. Control. Release*, 1998, **54**, 167.

93 N. Faisant, J. Siepmann, J. P. Benoit, *Eur. J. Pharm. Sci.*, 2002, **15**, 355.

94 V. Khare, S. Kour, N. Alam, R. D. Dubey, A. Saneja, M. Koul, A. P. Gupta, D. Singh, S. Singh, A. K. Saxena, P. N. Gupta, *Int. J. Pharm*, 2014, **470**, 51.

95 B. Narashimhan, S. K. Mallapragada and N. A. Peppas. Release kinetics, data interpretation. in: Encyclopedia of Controlled Drug Delivery. 3rd Eds. John Wiley and Sons Inc, New York; 1999.

96 N. A. Peppas, *Pharm. Acta Helv.*, 1985, **60**, 110.

97 T. Higuchi, *J Pharm Sci.*, 1963, **52**, 1145.

98 R. Bhaskar, S. R. S. Murthy, B. D. Miglani and K. Viswanathan, *Int. J. Pharm.*, 1986, **28**, 59.

99 A. Albanese, P. S. Tang, W. C. Chan, *Annu Rev Biomed Eng.,* 2012, **14**, 1.

100 B. Jakubíková and F. Kovanda , *Chem. Listy* ,2010, **104** ,906.

101 F. Danhier , E. Ansorena , J. M. Silva ,R. Coco, A. L. Breton, *J. Control. Release,* 2012, **161**, 505.

102 R. G. Stoller, K. R. Hande, S. A. Jacobs, S. A. Rosenberg and B. A. Chabner, *New Engl. J. Med.*, 1977, **297**, 630.

103 L. M. Kaminskas, B. D. Kelly, V. M. McLeod, *Mol Pharm*, 2009, **6**, 1190.

104 S. J. Choi, J. M. Oh, J. H. Choy, *J Nanosci Nanotechnol,* 2010, **10**, 2913.

Graphical Abstract

Optimization of the process parameters for fabrication of polymer coated layered double hydroxide-methotrexate nanohybrid for possible treatment of osteosarcoma.

Sayantan Ray, Akhilesh Mishra, Tapan Kumar Mandal, Biswanath Sa and Jui Chakraborty*

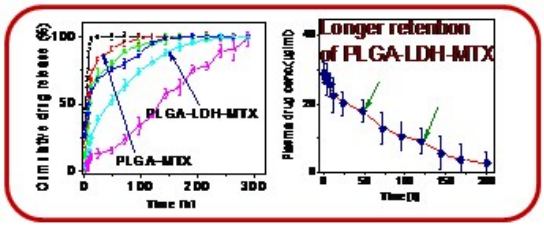

The study demonstrates the method of optimization for development of PLGA encapsulated LDH-MTX, MTX and their *in vitro* and *in vivo* evaluation.